The generation of Paneth-like cells in colorectal cancer to alter T-cell responses

Minn E Ng

St Hugh's College



A thesis submitted for the degree of Master of Science (by Research) in Oncology

Michaelmas Term 2022

Table of Contents

Abstract *4*

1 Introduction *6*

1.1 Colorectal cancer **6**

1.2 CRC and the tumour immune microenvironment **7**

1.2.1 CMS subtypes of CRC 7

1.2.2 MSI-H and MSS CRC immune phenotypes 8

1.3 Lymph node yield is associated with primary tumour immune response **10**

1.4 Paneth cells **13**

1.4.1 Paneth cells and CRC 14

1.4.2 Paneth cell differentiation 16

1.5 Hypothesis and aims **18**

2 Materials and Methods *19*

2.1 Cell line culture **19**

2.2 Cell line drug treatment **19**

2.3 *ATOH1* overexpression lipofectamine transfection **20**

2.4 SATB2 CRISPR-electroporation knockout **21**

2.5 Reverse transcription and RT-PCR **22**

2.6 Western blot **23**

2.7 Spheroid culture **24**

2.8 Flow cytometry **25**

2.9 IL2 ELISA **26**

2.10 Immunofluorescence **27**

2.11 *In-silico* analysis **28**

3 Results *31*

3.1 *In-silico* analysis **31**

3.1.1 Introduction 31

3.1.2 TCGA-based correlation matrix showed heterogeneity within Paneth cell populations. 32

3.1.3 Tumours with high *LYZ* and *DEFA5* expression elicit potentially different immune responses 33
3.1.4 Discussion 34

3.2 Drug compounds subtly induce secretory cell differentiation effects in 2D CRC cell line culture and 3D CRC cell line spheroids 39
3.2.1 Introduction 39
3.2.2 Wnt and Notch regulation affect differentiation status of CRC cell lines 40
3.2.3 Colorectal cancer spheroids have varying differentiation status 40
3.2.4 Discussion 41

3.3 *ATOH1*-overexpression induces *DEFA5*+ Paneth cell signature and causes Jurkat cell infiltration 45
3.3.1 Introduction 45
3.3.2 *ATOH1* overexpression induces *DEFA5* expression in SW480 2D and 3D spheroids 46
3.3.3 Jurkat cells as a model for T cell activation 48
3.3.4 *ATOH1*-overexpression enhances Jurkat cell infiltration and IL2 secretion 49
3.3.5 *ATOH1* overexpression in HT29 causes *DEFA5* level increase and inhibits spheroid formation 53
3.3.6 Discussion 56

3.4 SATB2-KO in SW480 induces *DEFA5* expression and Jurkat cell IL2 increase 58
3.4.1 Introduction 58
3.4.2 SATB2 knockout induces *DEFA5*+ Paneth cell differentiation 58
3.4.3 SATB2-KO increases Jurkat cell IL2 secretion 61
3.4.4 Discussion 62

4 Discussion 64

Acknowledgements 75

Bibliography 76

(14,599 words)

The generation of Paneth-like cells in colorectal cancer to alter T-cell responses

Minn E Ng
A thesis submitted for the degree of Master of Science (by Research) in Oncology
St Hugh's College, Michaelmas Term 2022

Immunotherapy in colorectal cancer (CRC), the third most diagnosed cancer worldwide, results in limited and unpredictable responses. There are two main molecular subtypes of CRC: microsatellite unstable and the more common microsatellite stable type. Microsatellite unstable CRC develops as a result of somatic or germline, genetic or epigenetic perturbations to DNA mismatch repair genes. Importantly, microsatellite stable cancers mostly respond poorly to immunotherapies due to their apparent lack of neoantigen presentation and immune infiltration. The main curative treatment of these cancers thus remains surgical resection of the tumour and adjacent lymph nodes with some patients then offered conventional chemotherapy. Traditional views propose the benefit of lymphadenectomy is to either prevent further spread of the disease from involved lymph nodes or to improve staging. However, a recent transcriptomic analysis from the Buczacki Group demonstrated a strong enrichment in adaptive immune response related gene sets associated with high lymph node (LN) yields. Given more immunogenic tumours are associated with better outcomes, these data suggest a tumour-intrinsic reason for the enhanced survival seen. Interestingly, our analysis also found signatures for Paneth cells were enriched in this high LN yield group. Paneth cells are a cell type found in the small intestine and only rarely in the large intestine, where colon cancer develops. In the small intestine they secrete antimicrobial peptides and regulate the inflammatory response. I hypothesise that

the presence of Paneth-like cells in colon cancer enhances the host immune response against the tumour. In this study, *in-silico* analysis revealed heterogeneity within Paneth cell populations in CRC, separating *LYZ*- and *DEFA5*-specific clusters. *ATOH1* plasmid overexpression and SATB2 CRISPR-cas9-knockout induced Paneth cell-specific *DEFA5* gene and protein expression in CRC cell lines and spheroids. Paneth cell differentiated models were co-cultured with Jurkat cells to test for immune effects. Co-culturing with *ATOH1*-overexpressing and SATB2-knockout cells caused an increase in spheroid infiltration and IL2 secretion of Jurkat cells. Therefore, I propose that differentiation therapy could potentially augment current immuno-oncology approaches by enhancing the host immune response against CRC.

1 Introduction

1.1 Colorectal cancer

Colorectal cancer (CRC) arises from the large intestine and rectum and is the third most diagnosed malignancy worldwide, with 1.93 million cases reported in 2020 and estimated new cases to reach 3.2 million globally in 2040 (Xi & Xu, 2021), causing a growing challenge to public health. CRC arises in the epithelium and is driven by three main genetic pathways. Chromosomal instability occurring in 65 - 70% of CRCs, is represented by prevalent aneuploidy, indels, translocations, amplifications, and loss of heterozygosity. These tumours are commonly associated with driver mutations in Adenomatous polyposis coli (*APC*), Kirsten rat sarcoma virus (*KRAS*), SMAD family member 4 (*SMAD4*), tumour protein P53 (*TP53*) (Pino & Chung, 2010). Secondly, inactivation of mismatch repair (MMR) genes e.g., *MLH1* and *MSH2* could result in a defect in the DNA MMR system and cause accumulation of microsatellite instability and is responsible for around 15% of CRCs. CRCs with microsatellite instability have high tumour mutation burden and display many immunogenic neo-antigens often correlated with better prognosis than MMR proficient tumours (Lin et al., 2020). Thirdly, the serrated neoplasia pathway, likely originating from *BRAF* V600E mutations, contributes to 15-25% of CRC. *BRAF* mutations lead to constitutive activation of the mitogen-activated protein kinase-ERK pathway, causing deregulation of cellular proliferation and division (Chan & Buczacki, 2021).

Recently, the conventional Vogelstein model which demonstrates a linear accumulation of driver mutations that drive the advancement of adenomas to invasive cancer, has been challenged by a 'big bang' evolutionary theory. The Volgelstein model argues for the continuous accession and clonal sweeps of *APC*, *KRAS*, *SMAD4* and *TP53* mutations in tumours (Fearon & Vogelstein, 1990). However, this should theoretically give rise to genetically homogenous and clonal tumours, whereas intra-tumoral heterogeneity is found a common hallmark of CRC. The big bang theory (Sottoriva et al., 2015) thus highlights that tumours generate intra-tumoral heterogeneity at premalignant stage through single intermixed expansion of emerging diverse subclonal populations. Then, a selected clone that overcomes growth limitations goes on to progress into advanced cancer in later tumourigenesis, and neutral evolution follows.

1.2 CRC and the tumour immune microenvironment

1.2.1 CMS subtypes of CRC

Due to large inter- and intra-patient heterogeneity, patients with CRC suffer varying and somewhat unpredictable clinical outcomes and drug treatment responses. Gene expression-based CRC subtyping reported four consensus molecular subtypes classifications (CMS) of CRC (Guinney et al., 2015). CMS1 included the majority of microsatellite unstable tumours (MSI-H). These had high tumour mutational burden with a high frequency of *BRAF* mutations, widespread hypermethylation and a defective DNA mismatch repair system. CMS2 subtype had a strong chromosomal instability phenotype, and displayed increased copy number variations. CMS3, with higher prevalence of *KRAS* mutations, conferred epithelial

and metabolic dysregulation. Lastly, CMS4 had upregulation of genes associated with epithelial-to-mesenchymal transition, transforming growth factor-beta signalling and increased angiogenesis. Upon gene set enrichment analysis (GSEA) of the four subtypes, CMS1 was revealed to have enhanced immune infiltrate including Th1 cells, cytotoxic T cells, natural killer (NK) cells and PD1 activation. In contrast, CMS2 subtype showed enrichment in Wnt and Myc downstream target genes but under enrichment of immune infiltration. CMS4 on the other hand had overexpression of proteins involved in stromal invasion and immune complement activation pathway (Guinney et al., 2015).

1.2.2 MSI-H and MSS CRC immune phenotypes

The tumour immune microenvironment plays an important role in both promoting or suppressing tumour growth. Several interactions between components of the immune system and tumour have been associated with prognosis and response to treatment in CRC. The MMR defect in MSI-H CRC (majority of CMS1 subtypes) leads to rapid introduction or deletion of nucleotides within genomic repeated regions and consequently results in frameshift mutations and thus neo-antigen formation that can be recognised by the immune system (Ionov et al., 1993). Hence, MSI-H CRC is often associated with an inflammatory tumour microenvironment with significant increase in the numbers of CD8+ T cells, CD4+ T cells, NK cells, M1 macrophages and neutrophils around the tumour (Guinney et al., 2015). These immune cells have anti-tumour properties and their presence associate with favourable prognosis. Similarly, expression levels of genes related to antigen presentation, cytolytic activity and interferon response are also upregulated in MSI-H cancers (Lin et al., 2020).

On the contrary, expression of immune checkpoint genes are upregulated in microsatellite stable (MSS) CRC, which accounts for 85% of CRC patients and the rest of the CMS subtypes (Lin et al., 2020). Recently, immune checkpoint inhibitors such as anti-PDL1 antibodies, have been shown to change the landscape of immune-epithelial interactions in several cancer types such as lymphoma, melanoma, renal cancer and lung cancer etc (Zhao et al., 2020). MSI-H CRC tumours have also showed good response to immune checkpoint inhibitor treatments such as Nivolumab (Overman et al., 2017) and Ipilimumab (Overman et al., 2018) and hence clinical benefit compared to MSS CRC. However, MSS tumours respond poorly to such therapies e.g. anti-PD-1 treatment, due to their lack of immune infiltration and recognition potential, insufficient mutant antigens, immune evasion and neovascularisation. Concordantly, MSS tumours represented low Th1 and cytotoxic T cell infiltration and elevated TGF-b levels (Lin et al., 2020).

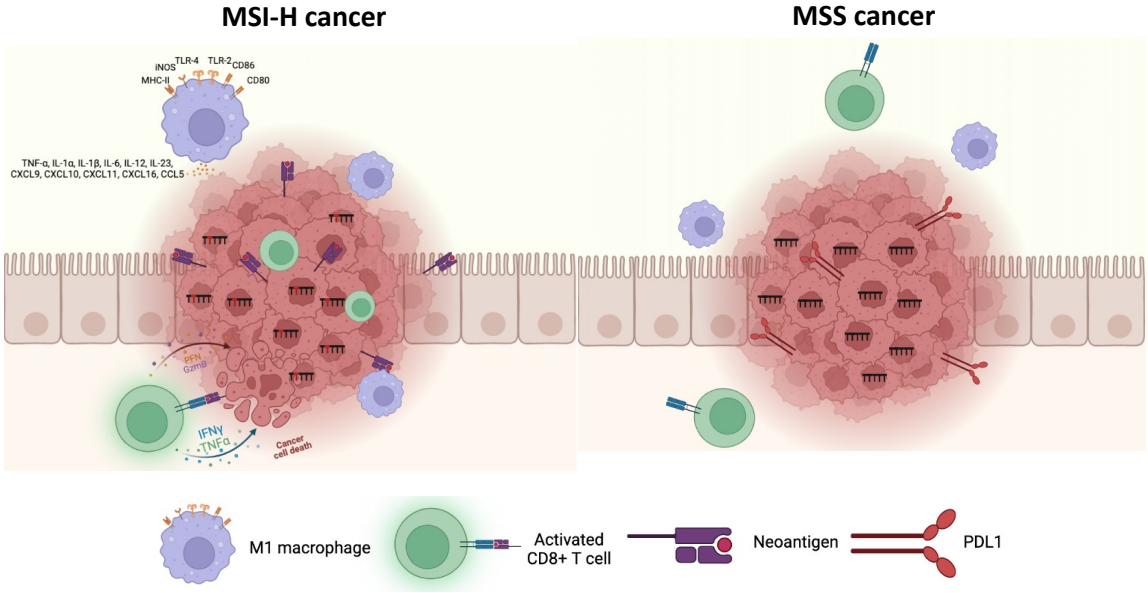


Figure 1.1 Immune infiltration of MSI-H versus MSS cancers.
MSI-H cancers (CMS1 subtype) have elevated neoantigen presentation, immune infiltration, cytokine signalling and tumour-killing. MSS cancers (CMS2, CMS3 subtypes) have greater immune checkpoint expression and lack of immune infiltration.
Image generated in Biorender.

Despite recent advances in understanding CRC biology, progress to improve immunotherapy and targeted therapy, particularly in MSS CRC remains stagnant. Therefore, the compelling goal in the CRC field is to investigate how MSS tumours can be made more responsive to immunotherapy to aid the destruction of tumour, or to find prognostic biomarkers to stratify patients in terms of their efficacy to respond to immunotherapy.

1.3 Lymph node yield is associated with primary tumour immune response

Seeing the lack of efficacy of immunotherapy and targeted therapy, the main curative treatment of CRC remains surgical resection of the tumour and adjacent lymph nodes (LN). Previous studies have shown that the number of LNs removed during surgical resection had significant association with survival outcomes, notably a high LN yield being associated with enhanced survival (le Voyer et al., 2003). Precise mechanisms and underlying reasons for this enhanced survival remain undefined. Traditional views suggest the reason for LN removal was to prevent further spread of the disease from these deposits to the lymphatic system (Halsted, 1907) or to improve staging (Foo et al., 2020; Sarli et al., 2005). Accurate staging is required for direction on long-term prognosis and importantly administration of adjuvant chemotherapy.

However, our recent multiomic analysis (Lal et al., 2022) revealed that LN yield in colon cancer is associated with primary tumour immune response. Our data confirmed a clear survival benefit with increased LN yield upon resections in both node-negative and node-positive MSS CRCs. By employing a ranked gene list of differentially expressed genes between high and low LN yield groups, the high LN yield dataset presented an enrichment in transcriptomic changes in genes sets such as INTERFERON_ALPHA_RESPONSE ($q<0.005$), INTERFERON_GAMMA_RESPONSE ($q<0.005$), ALLOGRAFT_REJECTION ($q<0.005$), and INFLAMMATORY_REPONSE ($q<0.005$). Interferon gamma is predominantly secreted by Th1 cells, CD8 cytotoxic T cells and natural killer cells. In cancer, upregulation of interferon gamma expression in CD4+ and CD8+ T cells enhances anti-tumour immunity by facilitating improved tumour recognition via stimulation of major histocompatibility complex molecules of tumour cells and antigen-presenting cells, as well as further T cells and NK cells trafficking (Du et al., 2021). Furthermore, interferon alpha, secreted by innate immune system is able to enhance tumour-killing. Importantly, our findings also concluded that the main differentially regulated processes between high and low LN yield colon cancer were the B- and T- cell adaptive immune responses (Table 1), and for the first time, we also described a strong association of dendritic cells with high LN yield tumours.

CELL SIGNATURE VS LN NEG - UPREGULATED GENES					
NAME	GS follow link to MSigDB	ES	NES	NOM p-val	FDR q-val
B-CELLS_NOVERSHTERN_2	B-CELLS_NOVERSHTERN_2	0.81829786	2.3930423	0	0
B-CELLS_NOVERSHTERN_1	B-CELLS_NOVERSHTERN_1	0.82927537	2.366363	0	0
B-CELLS_NOVERSHTERN_3	B-CELLS_NOVERSHTERN_3	0.841981	2.3470483	0	0
CD4+ T-CELLS_HPCA_2	CD4+ T-CELLS_HPCA_2	0.90191203	2.3168342	0	0
CD4+ T-CELLS_HPCA_3	CD4+ T-CELLS_HPCA_3	0.85698843	2.2893848	0	0
CD8+ TEM_BLUEPRINT_3	CD8+ TEM_BLUEPRINT_3	0.7895638	2.271392	0	0
NAIVE B-CELLS_HPCA_3	NAIVE B-CELLS_HPCA_3	0.8501962	2.267175	0	0
MEMORY B-CELLS_HPCA_2	MEMORY B-CELLS_HPCA_2	0.83918023	2.2514207	0	0
CD4+ T-CELLS_HPCA_1	CD4+ T-CELLS_HPCA_1	0.84301245	2.2400339	0	0
B-CELLS_HPCA_1	B-CELLS_HPCA_1	0.8218723	2.2265859	0	0

Table 1. B- and T-cell adaptive immune response enriched in high LN yield group.
The top 10 upregulated cell signatures in high LN yield group via GSEA, with majority involved in T cell and B cell signatures. ES: enrichment score, NES: normalised enrichment score, NOM p-val: normalised p-value, FDR q-val: false discovery rate-adjusted q-value. (Lal et al., 2022)

This unbiased bioinformatics analysis hypothesised that a strong primary immune response against tumour results in expansion of LNs that make them more visible during pathological analysis and thus easier to be retrieved. The enhanced survival in LN yield groups could therefore be explained by this greater lymphocytic involvement of the primary tumour (Fig 1.2A). Crucially, our data reported no association of LN yield with microsatellite stability nor CMS subtypes, revealing a tumour-intrinsic reason as to the enhanced immune response observed in the high LN yield group that is independent of mutational burden and MSI-high status of the tumour. These findings prompted our interest in investigating mechanisms behind this immune infiltration. Interestingly, further GSEA on ranked LN yield data revealed an enrichment in Paneth cell gene signatures including *LYZ, REG III* and *PLA2,* with *DEFA5* and *DEFA6* ranked within the top 4 genes in tumours with high LN yield (Fig 1.2B). We therefore speculated whether Paneth cells are responsible for this increased immune response.

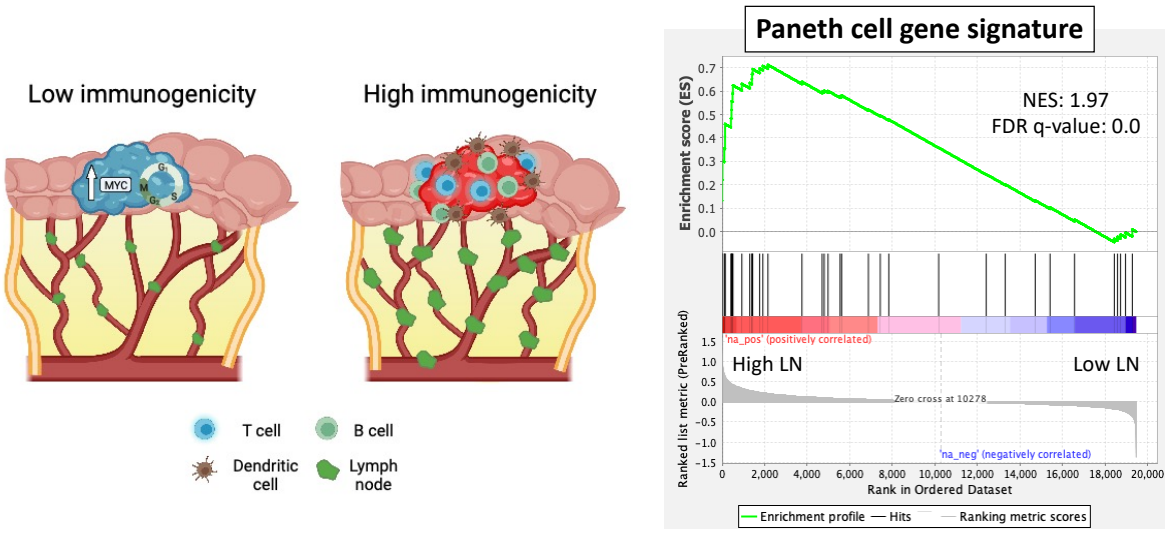


Figure 1.2 High LN yield tumours have enriched Paneth cell gene signatures.
(A) Tumours with higher LN yield revealed greater infiltration of T cells, B cells. (Lal et al., 2022)
(B) High LN yield tumours are correlated with high Paneth cell gene signatures.
NES: normalised enrichment score, FDR q-value: false discovery rate-adjusted q-value

1.4 Paneth cells

Paneth cells are a secretory epithelial population residing at the bottom of the small intestinal crypt, with about 5-15 cells per crypt. They are interspersed between intestinal stem cells and are responsible for the secretion of antimicrobial peptides to modulate the microbiome and regulate the inflammatory response in the small intestine. Paneth cells are traditionally known to also play a role in stem cell niche maintenance and proliferation by producing epithelial growth factors, Notch and Wnt signals to adjacent intestinal stem cells (Barreto e Barreto et al., 2022).

Besides its morphological distinct appearance with evident secretory granules, specific gene expression markers such as Lysozyme (*LYZ*) and Defensin alpha-5 (*DEFA5*) have also been extensively used to identify and characterise Paneth cells.

LYZ is an enzyme secreted by Paneth cells to hydrolyse peptidoglycans of bacterial cell walls. DEFA5 and Defensin alpha-6 (DEFA6) represent 70% of secreted peptides from Paneth cells. DEFA5 has lectin-like properties and permeabilises gram-positive and gram-negative bacterial membranes; DEFA6 self-assembles into nanofibril formations that entangle bacteria to prevent invasion into the epithelium (Bevins & Salzman, 2011). The secretion of these antimicrobial peptides allow regulation of intestinal microbiota and hence shape the community of immune system in the gut. Defensins that are secreted by Paneth cells have not only shown to be involved in antimicrobial functions but they also have direct immune regulatory roles. For example, Paneth cell secretions have been shown to cause chemotaxis of immature dendritic cells and cytokine production from epithelial cells (Ito et al., 2012). Additionally, the expression *DEFA5, DEFA6* and *LYZ* is significantly reduced in ileal Crohn's disease, with compromised Paneth cell function and number. This defensin-deficiency in inflammatory bowel diseases renders the patient more susceptible to uncontrolled intestinal inflammation (Wehkamp et al., 2005). It is therefore evident that Paneth cell antimicrobial peptides play a role in modulating the inflammatory response in the gut, however little research has been conducted to show molecular interactions between Paneth cells and their secretions, with the immune system, hence it is still uncertain how the crosstalk between Paneth cells and the immune system directly occurs.

1.4.1 Paneth cells and CRC

Although Paneth cells are normally found in the small intestine, they do not represent a population of bone fide epithelial cells in the colon. Prior investigations have proposed that they are instead replaced by cKit+ crypt base secretory cells in

the large intestine that have distinct transcriptional signature to Paneth cells, but also locate adjacent to intestinal stem cells to provide them with growth factors (Rothenberg et al., 2012). Nonetheless, few recent papers have reported the presence of Paneth cells in the rat ascending colon (Mantani et al., 2014) and even human large intestine (S. Gao et al., 2018). A greater effort has also been employed to explore the occurrence of Paneth cell metaplasia in different pathological conditions such as inflammatory bowel disease (Simmonds et al., 2014). In particular, the presence of Paneth cells and Paneth-like cell gene signature have long been associated with colorectal adenomas and adenocarcinomas (Holmes, 1965) and have been linked to the proximal colon and the male sex (Pai et al., 2013). However, the precise role of Paneth cells in CRC biology and immune phenotype, remains largely unknown and with contradictory findings.

Several papers have linked Paneth cell metaplasia with colonic tumourigenesis, with one stating that the accumulation of Paneth cells can be used as early prognosis to tumour malignancy (López-Arribillaga et al., 2021). In this study the authors showed that Paneth cell-positive adenoma areas are associated with increased Notch activity and Wnt/beta-catenin activation and may contribute to the activation of neoplastic stem cell signalling pathways in the early stages of carcinogenesis and hence reduced disease-free survival (López-Arribillaga et al., 2021). Furthermore, (X. Liang et al., 2022) found that disrupting *SOX9* activity (a gene that normally activates a Paneth cell transcriptional program) induces intestinal differentiation and impairs primary tumour growth. The presence of Paneth cells in early adenomas may be a marker for increased risk of developing colorectal neoplasia. (Pflügler et al., 2020) described that Stat1-dependent *Ido1* expression in

Paneth cells of intestinal tumours suppresses activation of CD8+ T cells and promotes regulatory T cell differentiation, favouring an immune-tolerant microenvironment and CRC progression in mice.

Conversely, (Mahon et al., 2016) a case study, suggested that there was an inverse association of Paneth cell presence and synchronous advanced adenoma, and Paneth cells can be used as a negative indicator of CRC development. Their findings suggested an alternative hypothesis, that Paneth cells may contribute to the suppression of CRC development. In summary, although contradictory, these studies showed that understanding the importance of Paneth cells in tumour promotion or tumour destruction, including their potential immune modulatory role, is non-trivial and precise mechanisms of their functions require further study.

1.4.2 Paneth cell differentiation

One of the major challenges of studying the role of human Paneth cells is their inability to be cultured singularly without the presence of other epithelial cells from the small intestine. More importantly, to fully understand the role of Paneth cell gene signature in the context of CRC, induction of Paneth cell formation in CRC models must be achieved. A major focus of this project was therefore to establish a method to mimic Paneth cell differentiation in CRC models.

A myriad of papers has demonstrated the role of several pathways in the regulation of secretory cell differentiation in normal murine and human small intestine. Firstly, several studies substantiated that Atonal BHLH Transcription Factor 1 (*ATOH1*) functions as a key transcription factor essential for intestinal secretory cell

differentiation. Its target genes include Notch ligands *DLL1* and *DLL4*; transcription factors such as *SOX9* and *GFI1*; and secretory lineage-specific genes such as *BEST2, SPINK4, MUC2, SCT, EPHB3, XBP1*, and *CLCA3* (Lo et al., 2017). The ablation of *Atoh1* gene in mice caused complete loss of Paneth cells (Durand et al., 2012a). Moreover, the environment in which Paneth cells reside is rich in Wnt. Wnt positively regulates *SOX9* and *ATOH1*, which upon upregulation, have also been known to specify secretory cell differentiation. Other factors such as YAP (Serra et al., 2019) and HMGA1 (Xian et al., 2017) also regulate *ATOH1* and *SOX9* expression via negative and positive regulation of the Wnt pathway, respectively. Conversely, an activated Notch pathway has been shown to have an inhibitory effect on secretory cell lineage promotion. Transcriptional Notch inactivation by protein kinase PKCλ/ι is required for Paneth cell differentiation by promoting transcriptional upregulation of *ATOH1* and *GFI1*, which drives Paneth cell fate (Nakanishi et al., 2016). Patients low in *PRKCI* that encodes PKCλ/ι is correlated with worse survival in CRC. PKCλ/ι deficiency increases Enhancer of zeste homolog 2 (EZH2) stability which represses *ATOH1* and *GFI1* expression and Paneth cell differentiation (Nakanishi et al., 2016).

In summary, these studies showed that a high concentration of Wnt with low supply of Notch creates a favourable environment for Paneth cell differentiation and SOX9 and ATOH1 are known transcription factors to regulate secretory lineage differentiation. Regulation of these factors *in vitro* could therefore create a Paneth cell phenotype in CRC models.

1.5 Hypothesis and aims

Our preliminary data revealed that patients with enhanced survival, correlated with high LN yield and elevated immune response, which is also associated with enrichment in Paneth cell gene signature. The specific role of Paneth cells / Paneth-like cells in CRC has yet to be explored and is an area of scant previous research. Although Paneth cells have an immune-modulatory role in the small intestine and inflammatory bowel disease, the role of Paneth cells on tumour immunogenicity particularly in CRC is an area requiring more attention. Polyps in the small intestine are rare but they commonly develop in the colon – the evident histological difference between the small intestine and large intestine are Paneth cells. The question thus arises: could Paneth cells play an immune-modulatory role in CRC?

Considering the role of Paneth cells in immune modulation and inflammation in the normal small intestine, I hypothesise that Paneth cell differentiation in CRC enhances the host immune response against the tumour. To investigate this, the first aim of my project was to establish a Paneth-like cell phenotype in CRC models using drug treatment, gene overexpression and CRISPR-knockout in CRC cell lines and spheroids. The next aim was to then use these Paneth-like cell models to investigate the role of Paneth cell gene expression on immune response. Jurkat cell co-culture assays were performed to determine the role of Paneth cells on immune response.

2 Materials and Methods

2.1 Cell line culture

Short tandem repeat genotyped and mycoplasma tested colorectal cancer cell lines (SW480, HT29 and RKO) were cultured in Dulbecco's modified Eagle's medium: Nutrient mixture F-12, no glutamine (Gibco, 21331020) supplemented with 10% heat-inactivated fetal bovine serum (Gibco, 10082147) and 1% Penicillin-streptomycin (Gibco, 15140122) at 37 °C in 5% CO_2. Cells were passaged at 70-90% confluency using TrypLE Express Enzyme no phenol red (Gibco, 12604021) after washing with DPBS (Sigma-Aldrich, D8537).

Jurkat cells were cultured in suspension and maintained in RPMI-1640 medium with L-Glutamine (Gibco, 11875093), supplemented with 10% HI-FBS (Gibco, 10082147), 1% Penicillin-streptomycin (Gibco, 15140122), and 50 µM 2-Mercaptoethanol (Gibco, 30350010). Cells were passaged every 3 days by removing parts of media containing cells and adding fresh media. When required, cells were stained with Trypan blue (Sigma-aldrich, T8154) and counted using the Luna II Automated Cell Counter (Labtech).

2.2 Cell line drug treatment

HT29, SW480 and RKO cells were seeded in an adherent 6-well plate (Starlab) and incubated at 37 °C in 5% CO_2. 24 hours later, drugs were added directly to the media at IC50 concentration obtained from the literature. All drugs were solubilised in DMSO. After 3 days of drug treatment, cells were trypsinised and cell pellets were harvested for subsequent analysis. RT-PCR was performed against *GAPDH* and *LYZ, DEFA5*, *MUC2*, *CHGA* differentiation markers.

Compound	Product	Final concentration to cells (μM)
CHIR99021	Tocris (Cat 4423)	3
DAPT	Alfa Aesar (Cas 208255-80-5)	10
GSK126	APExBIO (Cat A3446)	2
Valproic acid	Tocris (Cat 2815)	1000
Rapamycin	Tocris (Cat 1292)	7

2.3 *ATOH1* overexpression lipofectamine transfection

ATOH1 overexpression plasmid was purchased from Addgene (Cat# 162342), which was supplied in Escherichia coli. Plasmids were extracted using PureYield Plasmid Miniprep System (Promega, A1223), according to the manufacturer's manual.

HT29 and SW480 colorectal cancer cell lines were seeded in a 6-well plate at 0.25 - 1 x 10^6 cells per well. At 70-90% confluency, Lipofectamine 3000 transfection (Invitrogen, L3000001) was performed according to the manufacturer instructions. Briefly, DNA-lipofectamine complexes (DNA (2.5 μg/μL) diluted in P3000 reagent (2 μL/μg DNA) and Lipofectamine 3000 reagent (7.5 μL)) were prepared in Opti-MEM Reduced serum medium (Gibco, 31985062)) and added directly to cells in cell culture medium. After 24 hours of transfection, cells were treated with 0.1 μg/mL doxycycline (MP Biomedicals, 0219504401) to induce TetOn promoter. Following 24 hours of induction, fresh media was added and transfected cells were treated with 10 μM puromycin (Capricon Scientific, PUR-1X) selection. After 3 days, cells

were harvested, and RT-PCR performed against *GAPDH, ATOH1, DEFA5, LYZ, MUC2* and *CHGA* markers.

2.4 SATB2 CRISPR-electroporation knockout

CRISPR-cas9 knockout (KO) of SATB2 was performed using the Neon transfection system kit (Invitrogen, MPK10096). 1 x 10^5 cells were collected and resuspended in Resuspension buffer T. Resuspension buffer R, Cas9 protein (30 µM, Sigma-Aldrich, C120010) and sgRNA (100 µM) [Synthego CRISPRevolution sgRNA EZ kit (1.5 nmol) – SATB2 UGCUCCACGACACAAAAGAC] were added to the cells. sgRNA was designed using Synthego CRIPSR design tool. Electroporation was carried out using the Neon device, according to manufacturer's instruction using the below settings. Cells were directly added to media in a pre-warmed plate.

Setting	**Amount**
Voltage	1320 V
Width	30 ms
Pulse	1

Genomic DNA from KO-cells was isolated using Quick-DNA Miniprep Kit (Zymo Research, D3024) based on manufacturer's manual. Purified genomic DNA for knockout screens was PCR amplified using Q5 High-Fidelity DNA polymerase (New England Biolabs, M0491S) according to manufacturer's manual. 1000 ng of DNA was used in each 50 µL PCR reaction. SATB2 forward primer – TCGAGTGTCTGTGTGGTCACCT; SATB2 reverse primer – TGGGAGGAGAGGGGAGAGGCAT (IDT). Primers were designed using Benchling. PCR product was purified using QIAquick PCR purification kit (QIAGEN, 28104)

according to manufacturer's protocol and sent for Sanger sequencing (Genewiz). KO cells were single cell cloned using a serial dilution method to obtain clonal KO-population and once again confirmed by Sanger sequencing and Western blot.

2.5 Reverse transcription and RT-PCR

Total RNA was extracted from cell pellets using RNeasy Mini Kit (QIAGEN, 74104), according to manufacturer's instructions. Equivalent quantities of total RNA was measured using Nanodrop Spectrophotometer (Thermo Scientific Fisher) and were reverse-transcribed using the SuperScript VILO Master Mix (Invitrogen, 11755050). Complementary DNA (cDNA) was diluted with nuclease-free water and mixed with TaqMan Fast Advanced Master Mix (Thermo Fisher Scientific, 4444557) and appropriate Taqman probes listed below, then analysed by real-time PCR (StepOnePlus; Applied Biosystem). *ACTB* and *GAPDH* mRNA levels were used to normalise expression data using the ΔCt method in Excel and the data are presented as fold change calculated as $2^{Ct(housekeeping - gene\ of\ interest)}$.

qPCR Taqman probes: cat number 4331182

Gene	Code
GAPDH	Hs02786624
ACTB	Hs01060665
LYZ	Hs00426232
DEFA5	Hs00360716
MUC2	Hs03005103
CHGA	Hs00900370
ATOH1	Hs00944192
HLA-DR	Hs04192464
IL2	Hs00174114

IL2-RA	Hs00907777
CD69	Hs00934033

2.6 Western blot

Cells from a T25 flask were collected in ice cold PBS following TrypLE treatment. Cell pellets were lysed using Pierce RIPA lysis buffer (Thermo Fisher Scientific, 89901) with addition of Halt Protease and Phosphatase inhibitor single-use cocktail (Thermo Fisher Scientific, 1861280). Cells were sonicated for 20 seconds and left gently shaking on ice for 15 minutes then centrifuged at 20 000 x g for 7 minutes. Protein concentration was quantified using Pierce BCA protein assay (Thermo Fisher Scientific, 23225) according to manufacturer's instructions. NuPAGE LDS sample buffer (Life technologies, NP0008) plus NuPAGE sample reducing agent (Life technologies, NP0009) were added to lysates and samples heated at 70°C for 10 minutes. 20 µg of protein was loaded unto NuPAGE 4-12% Bis-Tris Gel (Invitrogen, NP0335BOX) submerged in NuPAGE MES SDS Running buffer 20X (Life technologies, NP0002). The XCell SureLock Mini- Cell (#EI0001, Thermo Fisher Scientific) was used for electrophoresis and ran at 180V for 50 minutes, along with Blue Prestained Protein Marker, Broad Range (Cell Signalling Technology, 59329). After electrophoresis, proteins were transferred at 20V for 45 minutes unto Nitrocellulose membrane (Invitrogen, LC2001) using NuPAGE transfer buffer 20X (Invitrogen, NP00061). Ponceau S staining (Tocris, 5225) for 1 minute was carried out to confirm presence of protein bands and quickly washed away with DPBS. Membrane was blocked for an hour with 5% skimmed milk (Serva, 42590.02) in Tris Buffered Saline, with Tween 20 (Sigma-Aldrich, 1002985083). Membranes were then incubated with primary antibodies anti-SATB2 (1:1000,

Abcam ab92446) in blocking buffer and anti-GAPDH (1:10 000, Thermo Fisher Scientific, MA5-15738) in 5% bovine serum albumin in TBST overnight at 4°C. The next day, membrane were washed with TBST and incubated with secondary anti-mouse (Cell Signalling Technology, #7074) and anti-rabbit (Abcam, ab205718) HRP conjugated antibodies at 1:10 000 dilution in TBST for an hour at room temperature. ECL Prime Western Blotting System (Sigma-Aldrich, Cytiva GERPN2232) was used to stain blot and Biorad chemiluminescence protocol used to scan image.

2.7 Spheroid culture

Cells were passaged and cell count performed (cell viability >90%). 2000 cells were seeded in 100 µL media suspension in each well using either ultra-low attachment 96-well round bottom plates (Corning 7007, 10023683) or Nuclon Sphera-Treated, U-shaped-bottom microplate (Thermo Fisher Scientific, 174925). Plate was centrifuged at 1500 rpm for 10 minutes at room temperature to initiate formation of spheroids. Spheroids were incubated at 37°C in 5% CO_2 at all times during experiments. A day after seeding, 100 µL media was added to each well containing spheroids. Media of spheroids can be changed by removing 100 µL from each well and adding 100 µL fresh media, without disrupting the spheroids. Spheroids were allowed to grow for at least 4 days before any assays were performed.

ATOH1-overexpressing and SATB2-KO spheroids

For *ATOH1* overexpressing spheroids, cells were transfected with *ATOH1* plasmid as described above and following puromycin selection, cells were trypsinised and counted. 12 wells of spheroids were seeded for each transfection. SATB2-KO cells

were also seeded as 12-well replicates. All spheroids were seeded in RPMI medium (due to convenience of coculture with Jurkat cells).

RNA extraction of spheroids

To extract total RNA from spheroids, 12 wells of spheroids per condition were pooled and harvested into a 1.5 mL Eppendorf. The spheroids were spun down and TrypLE was added, and cells incubated for 6 minutes at 37 °C. Samples were centrifuged at 300 x g for 5 minutes and cell pellets were used for subsequent analysis.

Spheroid and Jurkat cell co-culture

Prior to coculture, Jurkat cells were stimulated with 50 ng/mL PMA (Sigma-Aldrich, 16561-29-8) and 1 µg/mL Ionomycin (Santa Cruz Biotechnology, 56092-82-1). For coculture, 100 µL of spheroid media was removed and 8000 Jurkat cells (either stimulated or unstimulated) in 100 µL media were added to each well of spheroids. Cocultures were incubated at 37 °C for 24 hours. For flow cytometry and ELISA analyses, 12 wells per condition were seeded and either cells or supernatant were pooled from the 12 wells per replicate.

2.8 Flow cytometry

Each sample / coculture was transferred to a 1.5 mL Eppendorf, centrifuged, and pelleted. DPBS (Gibco, 14040133) was used for all washing steps. Human TruStain FcX blocking antibody (1:100, BioLegend, 422302) was added at 1:100 dilution and samples incubated at room temperature for 5-10 minutes. Without washing, primary antibodies were added at 1:100 dilution and samples incubated at 4°C for 30

minutes in the dark. Violet 711 CD25 (BioLegend, 356138), Alexa Fluor 647 CD69 (BioLegend, 310918), Violet 421 PD1 (BioLegend, 329920), LIVE/DEAD Fixable Near IR Viability stain (Invitrogen, L34992). Antibody concentrations were determined via previous pilot titration experiments. After incubation, cells were washed and fixed with 4% paraformaldehyde. To prepare compensation beads for each fluorophore, antibodies were added to 2 drops of beads in a 1:100 dilution and incubated at 2-8°C for 15-30 minutes in the dark. DPBS was added and beads centrifuged at 500 x g for 5 minutes, then resuspended in FACS buffer. FACS Attune machine was used to run samples. Forward and side scatter was determined, and compensation beads used to determine compensation and running voltages. Results were analysed on Flowjo software. FMO controls were used to gate for GFP+, CD25+, PD1+ and CD69+ populations.

2.9 IL2 ELISA

Following co-culture, suspended cells in the media were spun down and supernatant retrieved. Samples were stored at -20°C until ready to be assayed. IL2 ELISA (Invitrogen, BMS221-2) was performed according to manufacturers' manual. Briefly, 2D coculture samples were diluted with media at a 1:1000 dilution and 3D coculture samples were directly used. Biotin-conjugate, Streptavidin-HRP, TMB substrate solution was added sequentially after appropriate incubation times. When reaction is completed, stop solution was added to each well and absorbance at 450 nm was measured immediately using the POLARstar OMEGA microplate reader. Standard curve was produced and extrapolated in Graphpad prism to obtain final concentration values.

2.10 Immunofluorescence

Immunofluorescence of *ATOH1*-overexpressing and SATB2-KO cells

Cells were seeded in µ-Slide 8 well high chambered coverslips (Ibidi, 80806) at 20,000 cells per well. After 24 hours of incubation at 37°C, cell culture medium was aspirated from the wells and cells washed with DPBS and fixed with 4% formaldehyde (Thermo Scientific, 28908) for 20 minutes. 0.1% Triton X-100/PBS (Sigma-Aldrich, 9036-19-5) was used to permeabilise cells for 10 minutes and then cells were blocked with 1% BSA blocking solution/0.1% PBS-Tween20 (Sigma-Aldrich, 9005-64-5) for 30 minutes. Primary antibodies were diluted in 1% BSA blocking solution and incubated with cells overnight at 4°C. The next day unbound primary antibodies were washed away with DPBS and slides incubated with secondary antibody for 1 hour at room temperature in the dark. DAPI (1 µg/mL, Thermo Scientific, 62248) was used for nuclear staining. Mounting medium (Ibidi, 50001) was added directly into the chambered slides. Images were taken using the Zeiss 710 microscope and analysed on ImageJ Fiji.

Immunofluorescence of OCT-frozen colon and small intestinal human tissue samples

All human tissue samples obtained were from research consented patients, REC number 21/YH/0206. Tissue samples were fixed in 4% formaldehyde for 48 hours at room temperature then transferred to 20% sucrose (in water) at 4°C for a further 48 hours. Samples were then embedded in OCT medium and sectioned by the Oxford Centre for Histopathology Research (University of Oxford). Frozen sections were washed with PBS to remove OCT. Slides were covered in 1% SDS for 5 minutes for antigen-retrieval. 0.05% PBS-Tween20 was used for all washing steps.

Sections were blocked with 5% BSA (in PBS-T) for 30 minutes. Primary antibodies were incubated at room temperature for an hour. Unbound primary antibodies were washed away with PBS-T and slides incubated with secondary antibodies for an hour at room temperature in the dark. DAPI nuclear stain (1 µg/mL) was added, and mounting medium dropped before a coverslip was applied. Images were taken using the Zeiss 710 microscope and analysed on ImageJ Fiji.

Primary antibodies – Anti-Lysozyme Mouse Monoclonal Antibody (Thermo Fisher Scientific, MA1-82873, 1:100) and Polyclonal Rabbit Anti-DEFA5 Antibody (Atlas antibodies, HPA015309, 1:100).

Secondary antibodies – Alexa Fluor 594 conjugated goat anti-mouse IgG (H + L) $F(ab')_2$ (Cell Signaling Technology, #8890S, 1:200), Alexa Fluor 488 conjugated goat anti-rabbit IgG (H + L) $F(ab')_2$ (Cell Signaling Technology, #4412, 1:500), DyLight 405 AffiniPure goat anti-mouse IgG (H + L) (Jackson ImmunoResearch, 115-475-003, 1:400).

2.11 *In-silico* analysis

SATB2 volcano plot

Dataset was retrieved from cBioportal – Colorectal Adenocarcinoma (TCGA, PanCancer Atlas). Gene co-expression data for differentiation markers *LYZ, DEFA5, MUC2* and *CHGA* was retrieved. Spearman correlation values between differentiation markers and chromatin modifier genes were analysed in Excel. Genes that were significantly negative or positively correlated to *LYZ, DEFA5, MUC2* and *ATOH1* (q-value < 0.05) were filtered and highlighted. Volcano plot was generated using Graphpad prism v9.

Correlation matrix and hierarchical clustering

This work was kindly assisted by Dr Amit Mandal (Lee Placito Fellow in Bioinformatics, Nuffield Department of Surgical Sciences). Expression (gene counts) were downloaded from NCI-GDC data portal. Only samples of the primary tumour, no prior treatment history, colon adenocarcinoma tumour type, non-FFPE were retained. All other sub-types or tissue origin if rectal were removed and samples with non-unique ID at 16-character level were eliminated. Before proceeding for normalisation, basal level genes were removed. The threshold used was that any gene should have at least value of count 5, in >5% samples. Normalisation was performed using limma-voom method with the following parameters – estimated library size was given as adjustment factor, the tissue source site and the sample shipment date were obtained and given as adjustments factors. Batch-effect was removed using SVA method.

Paneth cell markers list was obtained from panglaoDB [https://panglaodb.se/markers.html?cell_type=%27Paneth%20cells%27].

Correlation plot showing how expression of Paneth cell genes correlated with one another was generated using the Corrplot package on R studio. Hierarchical clustering was performed using clValid package on R studio.

Gene set enrichment analysis

Gene set enrichment analysis (GSEA) was performed on transcriptomic data ranked for expression of *LYZ, DEFA5, MUC2, CHGA* and *ATOH1*, obtained from cBioportal, against the 'hallmark' gene sets in GSEA v4.1.2 software package.

ImageJ Jurkat cell counting

Area of spheroids and sphericity index were measured in ImageJ using macro downloaded from [**https://doi.org/10.1371/journal.pone.0103817**]. The resulting shape of spheroid was annotated, image inverted and selected as 8-bit image to reveal individual cells. A plugin for cell nuclei counting was downloaded from [https://bioimage.ucsb.edu/docs/automatic-nuclei-counter-plugin-imagej]. Width - 5, minimum distance - 2.5, threshold – 1, parameters were used to count the number of GFP-positive Jurkat cells within the spheroid.

Statistical analysis

All statistical analyses were performed in Graphpad prism software v9. All data were assessed for normality using the D'Agostino and Pearson test, and Shapiro-Wilk test. Significance of parametric data were tested using an unpaired Student's *t* test and the Mann Whitney *U* test was used for nonparametric data. For multiple group comparisons, ANOVA testing was performed.

3 Results

3.1 *In-silico* analysis

3.1.1 Introduction

The majority of present research defined Paneth cells via their morphological presence i.e. secretory granules and through positive immunohistochemical staining for the Paneth cell marker LYZ (López-Arribillaga et al., 2021). However, a recent single-cell RNA-sequencing study (Burclaff et al., 2022a) on healthy human adult small intestine and colon epithelium suggested that although the murine specific Paneth cell marker *LYZ* is present in human Paneth cells, it is not restricted to solely Paneth cells in the human small intestine, and rather is most highly expressed in novel BEST4+ cells. Further, the gene signature of rare human colonic Paneth-like cells has not been described. Therefore, this prompted a comprehensive investigation of the expression levels of all Paneth cell-related gene signatures in normal human colon and CRC.

Various databases allow the investigation of gene expression in cancer tumours. Of those, The Cancer Genome Atlas (TCGA) represents a robust and comprehensive platform for genomic and molecular characterisation of many cancers including colorectal cancer (Z. Wang et al., 2016). Therefore, expression data in TCGA was used to define Paneth cell gene expression in CRC.

3.1.2 TCGA-based correlation matrix showed heterogeneity within Paneth cell populations

A correlation matrix was performed for both colon adenocarcinoma and normal colon for Paneth cell gene expression data obtained from TCGA. Batch effects were removed and expression markers for Paneth cells of each tumour and normal sample were compared with each other. Some goblet cell and enteroendocrine cell markers were also included.

Correlation matrix demonstrated that although the main Paneth cell specific markers *DEFA5* and *DEFA6* were well correlated in both normal and CRC samples, *LYZ* and *DEFA5* were not well correlated in either normal colonic tissue (Fig 2A) nor cancer (Fig 2B). Hierarchical clustering and subsequent clustering validation analyses revealed two distinct clusters of Paneth cell gene signatures in TCGA CRC data. One cluster associated with *LYZ* and *MMP7* expression, and another with *DEFA5*, *DEFA6* and *ATOH1*. For normal colon data, hierarchical clustering still demonstrated two distinct clusters, albeit *ATOH1*, *DEFA5* and *DEFA6* being more closely related to *LYZ*, with a shorter clade height difference.

To validate these findings, frozen sections of human biopsies of normal small intestine and colon were stained for LYZ and DEFA5 proteins. In the small intestine, as expected, DEFA5 and LYZ were well correlated and co-localised in the known location of Paneth cells at the bottom of intestinal crypts, even though DEFA5 staining was found to be of higher intensity than LYZ (Fig 2C). In the colon, although not located at the common Paneth cell residence at the bottom of the crypts, DEFA5 protein staining was still observed indicating some expression of *DEFA5* even in

normal colon (Fig 2C), possibly referring to the colonic Paneth-like cells. Interestingly here, LYZ did not co-localise to DEFA5, reflecting possible heterogeneity of Paneth cell gene expression in the colon with this heterogeneity being potentially amplified in CRC, according to my *in-silico* analyses. To advance this work in the future, further staining on the small intestine and colon of two other patients including haematoxylin and eosin staining from paraffin embedded matched sections could be included.

3.1.3 Tumours with high *LYZ* and *DEFA5* expression elicit potentially different immune responses

The differential expression patterns of *LYZ* and *DEFA5* was surprising and led me to question whether the distinct Paneth cell gene expression is able to contribute to immune response differently in CRC, considering the role of these antimicrobial peptides on immunomodulation in healthy small intestine. Therefore, the log ratio of gene expression level of *LYZ* and *DEFA5* were ranked for CRC samples using cBioPortal, which is a web-based platform for cancer genomic datasets from over 20 cancer studies (Cerami et al., 2012; J. Gao et al., 2013), and GSEA was performed against hallmark gene sets. Notably, *LYZ*-high samples were negatively correlated with interferon gamma, interferon alpha and inflammatory response (Fig 2D). On the contrary, a higher *DEFA5* expression level showed strong positive enrichment of interferon gamma and interferon alpha response (Fig 2E). This concurs with the strong positive correlation in interferon gamma and alpha response in tumours that have enrichment in Paneth cell gene signatures in the high LN yield group as previously described (Lal et al., 2022). It is worth noting that *DEFA5* appeared as the top 2 gene enriched in the high LN yield group, whereas *LYZ* was

further down the list at number 15 in our previous GSEA analysis between high and low LN yield group (Lal et al., 2022).

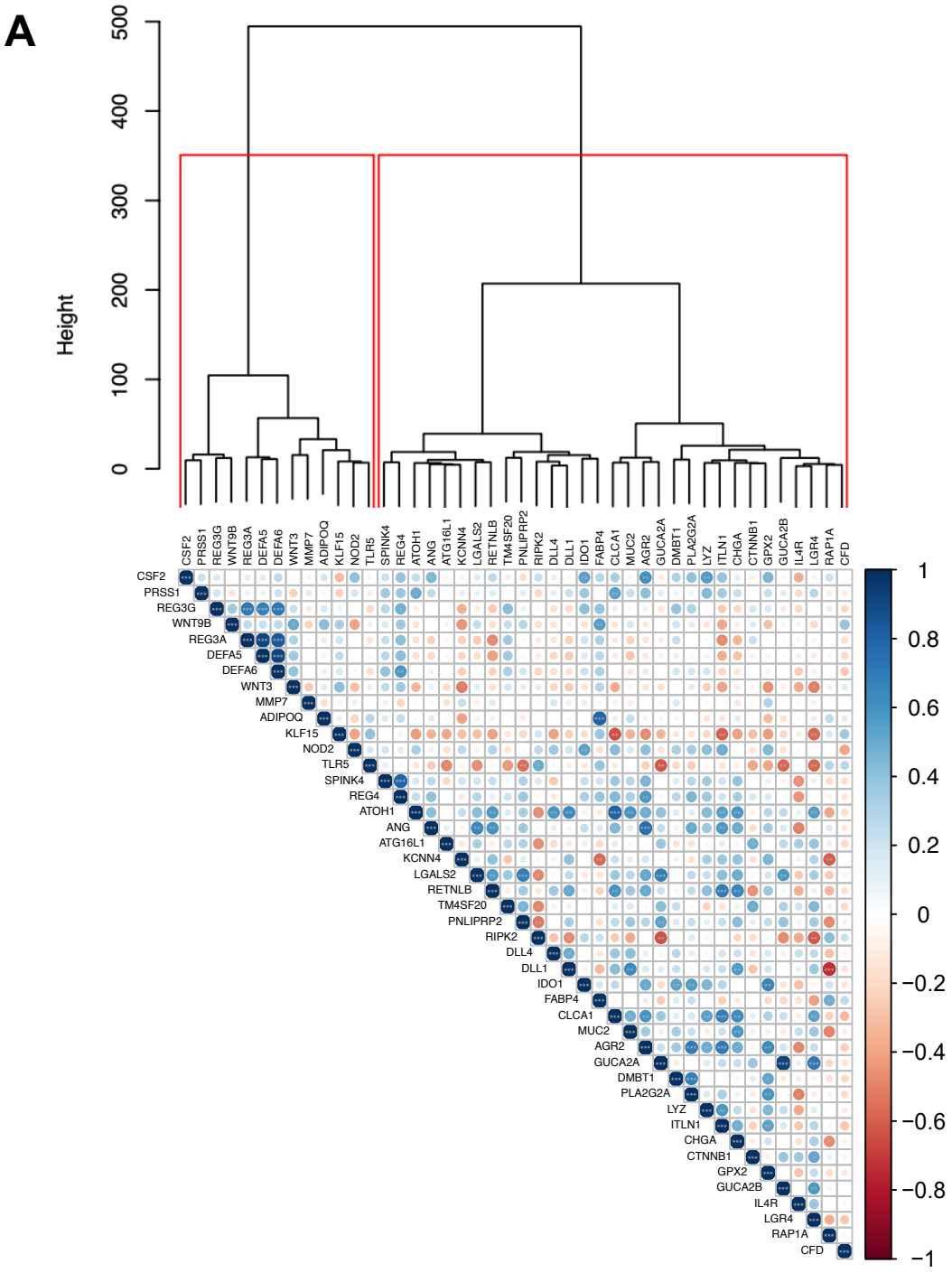
3.1.4 Discussion

Overall, although the conventional view is for small intestinal Paneth cells to highly express both *LYZ* and *DEFA5*, I showed here that there is heterogeneity between Paneth cell populations in the normal human colon and in the context of CRC, which has not been previously described. Of note, strong positive or negative correlations seen in normal tissue also seemed to be less prominent in cancer tissue (Fig 2A, B). Given tumours are transcriptionally more heterogeneous any correlations might be diluted within these samples compared to normal tissue. The sample size of normal colon data is also smaller hence differences might be amplified.

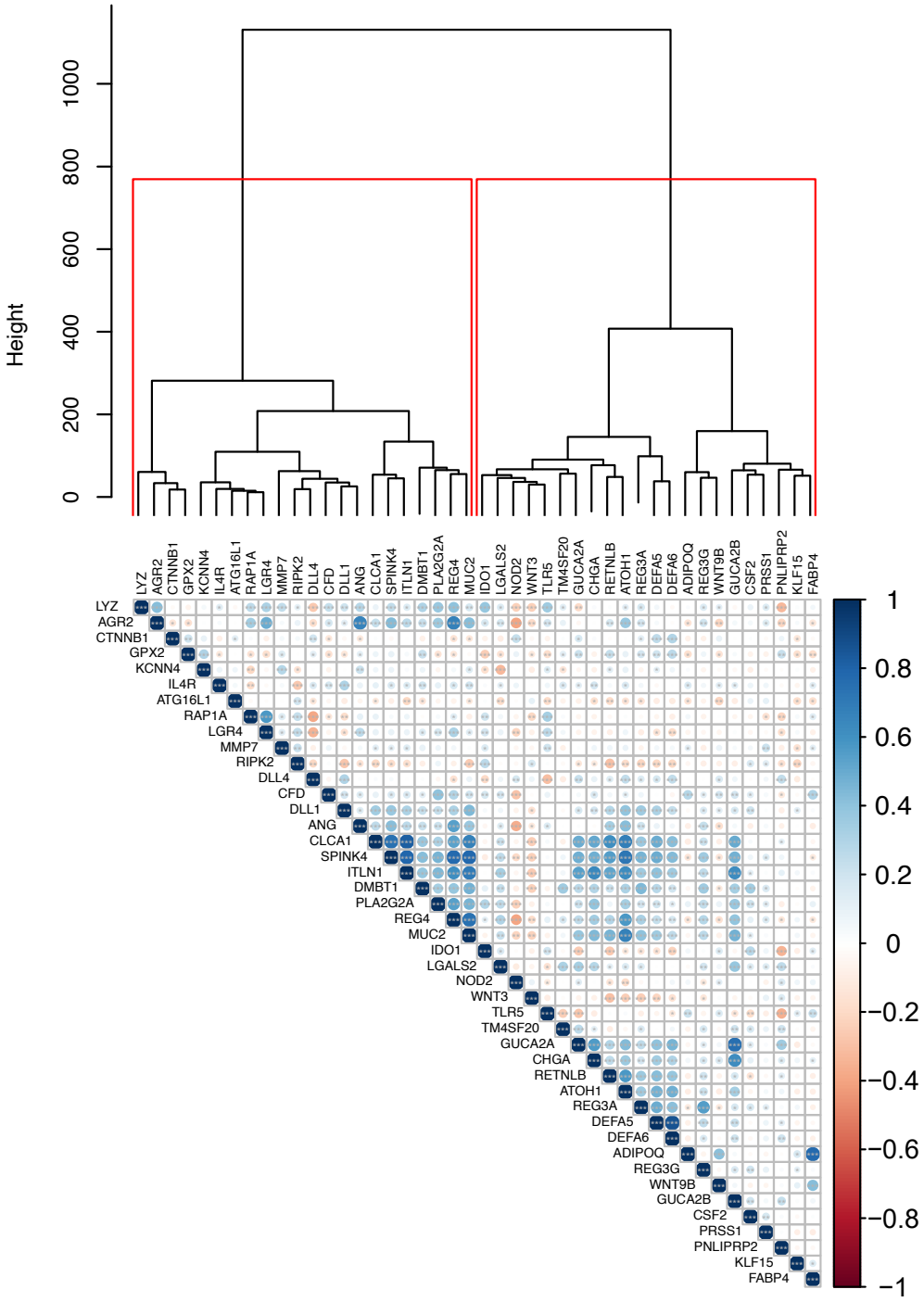
Interferon gamma and alpha responses are crucial to bridge innate and adaptive immunity for full activation against the tumour. The release of interferon gamma is indicative of a fully activated adaptive immune response, to mediate pathogenic clearance (Martin-Hijano & Sainz, 2020). It appeared here that *DEFA5* but not *LYZ* expressing tumours might be associated with enhanced immune response. A recent paper proposed that IDO1+ Paneth cells promote immune escape in CRC (Pflügler et al., 2020). In the study and concordantly in my analysis, *IDO1* was positively correlated with *LYZ* in both normal and cancer. Interestingly, *IDO1* was also positively correlated with *DEFA5* and *DEFA6* in normal tissue (Fig 2A) but negatively correlated in cancer (Fig 2B). I therefore hypothesise that the heterogeneity of Paneth cell gene expression present in CRC might play a role in the disparate tumour immunogenicity in patients. Although *LYZ*-expressing cells

promote immune escape, *DEFA5*-expressing cells in the tumour potentially enhance host immune response against the tumour.

I began to analyse published single cell sequencing datasets (Burclaff et al., 2022b; Pelka et al., 2021) to validate my bulk RNA sequencing and immunofluorescence analyses, and in the hopes to identify specific genes that regulate *LYZ*- and *DEFA5*-specific expression, however I did not have time to complete these analyses.


A
Height
0
100
200
300
400
500
CSF2
PRSS1
REG3G
WNT9B
REG3A
DEFA5
DEFA6
WNT3
MMP7
ADIPOQ
KLF15
NOD2
TLR5
SPINK4
REG4
ATOH1
ANG
ATG16L1
KCNN4
LGALS2
RETNLB
TM4SF20
PNLIPRP2
RIPK2
DLL4
DLL1
IDO1
FABP4
CLCA1
MUC2
AGR2
GUCA2A
DMBT1
PLA2G2A
LYZ
ITLN1
CHGA
CTNNB1
GPX2
GUCA2B
IL4R
LGR4
RAP1A
CFD
1
0.8
0.6
0.4
0.2
0
−0.2
−0.4
−0.6
−0.8
−1

B


Height
0
200
400
600
800
1000
LYZ
AGR2
CTNNB1
GPX2
KCNN4
IL4R
ATG16L1
RAP1A
LGR4
MMP7
RIPK2
DLL4
CFD
DLL1
ANG
CLCA1
SPINK4
ITLN1
DMBT1
PLA2G2A
REG4
MUC2
IDO1
LGALS2
NOD2
WNT3
TLR5
TM4SF20
GUCA2A
CHGA
RETNLB
ATOH1
REG3A
DEFA5
DEFA6
ADIPOQ
REG3G
WNT9B
GUCA2B
CSF2
PRSS1
PNLIPRP2
KLF15
FABP4
1
0.8
0.6
0.4
0.2
0
−0.2
−0.4
−0.6
−0.8
−1

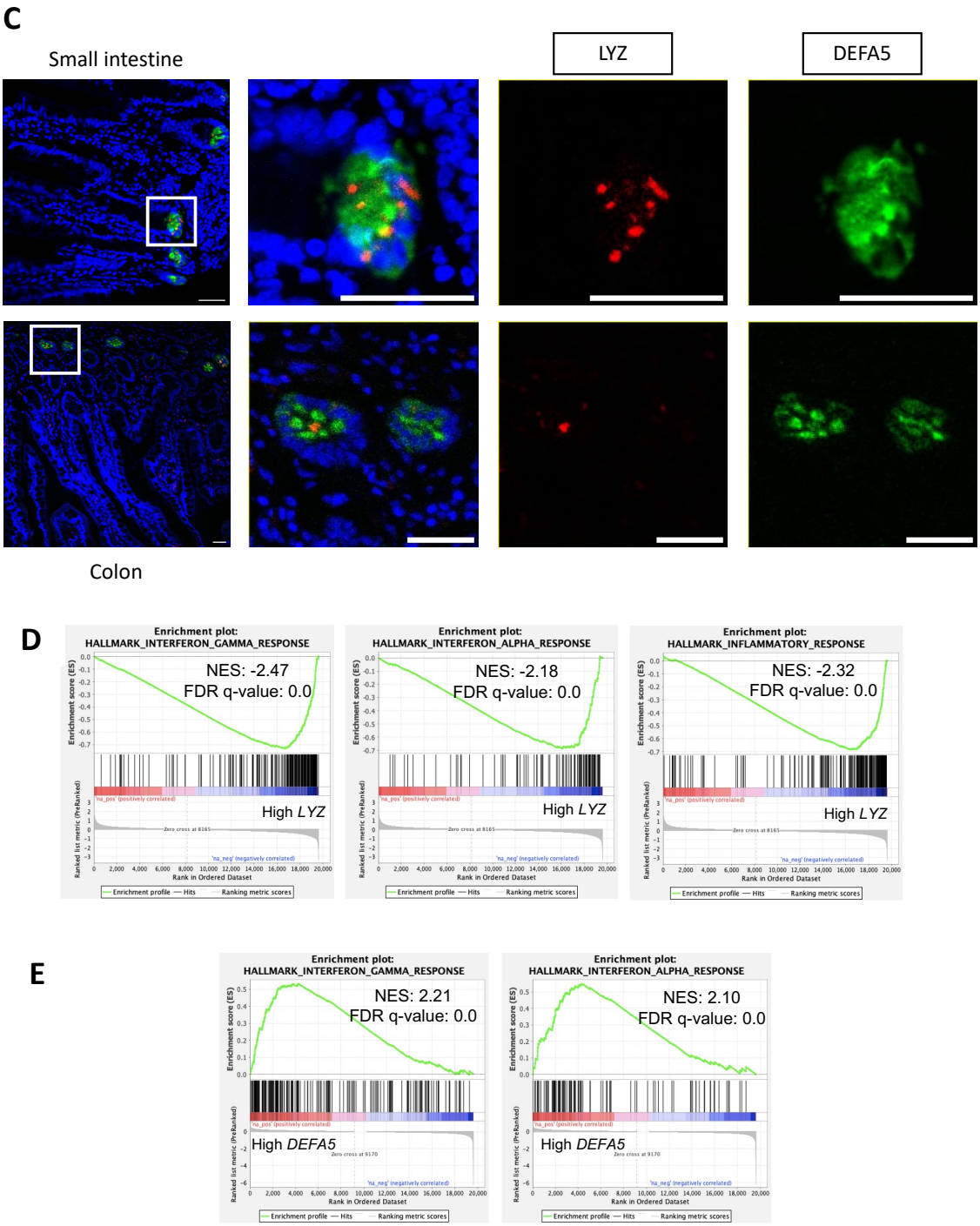


Figure 2. Heterogeneity within Paneth cell populations in normal colon and CRC tumours, showing differential *LYZ* and *DEFA5* gene expression.

(A, B) Correlogram of TCGA expression data for Paneth cell-associated gene markers in normal colon (A) and CRC (B), with dendrogram representing hierarchical clustering. *P< 0.05, **P< 0.0001, ***P< 0.00005.

(C) Immunofluorescence staining of frozen sections of small intestine (top) and colon (bottom) for DAPI (blue), LYZ (red) and DEFA5 (green). Scale bar: 50 μm

(D, E) GSEA showing the gene activity of immune responses for *LYZ* ranked (D) and *DEFA5* ranked (E) CRC samples obtained from TCGA expression data. NES = Normalised enrichment score, FDR q-value = False Discovery Rate – q-value normalised for multiple testing

3.2 Drug compounds subtly induce secretory cell differentiation effects in 2D CRC cell line culture and 3D CRC cell line spheroids

3.2.1 Introduction

To investigate the role of Paneth cells, a Paneth-like cell phenotype has be to established in CRC *in vitro* models. Previous studies have reported achieving secretory cell differentiation using several drug compounds targeting the secretory cell differentiation pathways. These were mostly performed in human normal small intestinal and colonic organoids, and also in mice (A. Treveil et al., 2020; Farin et al., 2012; Nakanishi et al., 2016; Yin et al., 2014). 6-[[2-[[4-(2,4-Dichlorophenyl)-5-(5-methyl-1H-imidazol-2-yl)-2-pyrimidinyl]amino]ethyl]amino]-3-pyridinecarbonitrile (CHIR99021), N-[N- (3,5-difluorophenacetyl)-L-alanyl]-S-phenylglycine t-butyl ester (DAPT), GSK126, Rapamycin and Valproic acid (VPA) were noteworthy compounds with previously reported abilities to target various components of the Paneth cell differentiation pathway (Fig 3A). CHIR99021 is a glycogen synthase kinase 3b inhibitor that prevents b-catenin degradation, thus keeping the Wnt pathway active; DAPT is a gamma-secretase inhibitor which blocks Notch signalling; and VPA is a histone deacetylase inhibitor with roles in Notch activation (Yin et al., 2014). GSK126 is a high affinity and selective inhibitor of the methyltransferase enzyme EZH2, known to have epigenetic control of *ATOH1* (Nakanishi et al., 2016) and Rapamycin is a mTOR inhibitor where mTORC1 signalling has also been shown to influence Paneth cell numbers (Yilmaz et al., 2012). Therefore, the first aim here was to treat MSS and MSI-H cancer cell lines with these compounds and quantify Paneth cell differentiation.

3.2.2 Wnt and Notch regulation affect differentiation status of CRC cell lines

CHIR99021, DAPT, GSK126, Rapamycin and VPA were administered to CRC cell lines SW480, HT29 and RKO. These drugs were tested individually and in combination for their role in inducing Paneth cell differentiation. mRNA levels of terminal differentiation Paneth cell markers *LYZ* and *DEFA5*; goblet cell marker Mucin-2 (*MUC2*) and enteroendocrine cell marker chromogranin A (*CHGA*) were measured following 3 days of drug treatment.

RT-PCR analyses demonstrated that the combination of GSK126 and DAPT caused a significant 4-fold increase in *LYZ* and average 38-fold increase in *DEFA5* mRNA levels in SW480 cell line compared to the DMSO control (Fig 3A). No significant differences in differentiation marker gene expression were observed when HT29 cell lines were treated with the compounds. For both SW480 and HT29, an increase in *MUC2* expression was noted when cells were treated with CHIR99021. HT29 treatment with DAPT alone and GSK126 alone also displayed a trend towards increased *MUC2* levels, albeit not statistically significant, likely due to variability in the results. *MUC2* is a marker specific for goblet cells, suggesting that there might be a potential increase in goblet cell numbers upon drug treatment. Furthermore, no increase in differentiation markers were seen between DMSO control and treated RKO cells. In fact, there was a significant decrease in *LYZ* expression in compound-treated samples (Fig 3A).

3.2.3 Colorectal cancer spheroids have varying differentiation status

SW480, HT29 and RKO cell lines were subsequently cultured in 3D suspension to form spheroids by centrifugal force. Spheroids are a better mimic of the 3D

environment in the human body and model some complexity of solid tumours (Costa et al., 2016). Surprisingly, SW480 spheroids showed a significant 46-fold increase of *DEFA5* expression relative to 2D culture (Fig 3B). HT29 spheroids showed a substantial increase in *MUC2* expression and a slight increase in *LYZ* expression compared to its 2D counterpart. A striking morphological difference was also observed between HT29 and SW480 spheroids. HT29 spheroids appeared smaller, more compact and cystic. Whereas at day 6 after seeding, SW480 spheroids were larger but individual cells still visible and appearing more sparse, mimicking a tight cell aggregate (Fig 3C). Similar to SW480, RKO spheroids appear to have a loose cell aggregate morphology (Fig 3C) and there was a slight increase in *ATOH1* expression in RKO spheroids, however no change in expression of terminal differentiation markers (Fig 3B). Intriguingly, when SW480 spheroids were treated with the combination of GSK126 and DAPT (which caused increased *LYZ* expression in 2D), the drastic increase of *DEFA5* in the spheroids was completely abolished. *DEFA5* and *LYZ* expression in spheroids were significantly reduced to levels comparable to 2D-cultured cells treated with the same drugs, based on evaluation of dCt values in RT-PCR (Fig 3D).

3.2.4 Discussion

SW480 had the biggest potential for Paneth cell differentiation through administration of GSK126 and DAPT amongst the three lines, of which HT29 was not influenced by compounds and opposite effects were seen in RKO. A recent study characterised SW480 cell line as more undifferentiated and expressed higher epithelial-to-mesenchymal and TGF-beta induced genes (Berg et al., 2017). I showed here that the combination of Wnt activation and Notch inhibition were able

to cause subtle differentiation in SW480. Although no differences were observed in the expression of terminal differentiation markers post-drug treatment, the baseline *LYZ* expression level in untreated HT29 cells was high, with raw Ct values similar to the housekeeping gene. (Berg et al., 2017) suggested that the HT29 cell line have more colon-like features with higher ability to differentiate into colon-like cells. My data suggested upregulation of *MUC2* upon drug treatments, demonstrating the ability of HT29 to differentiate into goblet cells, which are abundant in the human colon, rather than Paneth cells. On the other hand, unlike SW480 and HT29 which are MSS cell lines, RKO are MSI-H cells, and have also been classified as more undifferentiated (Berg et al., 2017), which was reflected in my results here in which drug treatments did not induce increased differentiation.

Furthermore, 3D culture of SW480, HT29 and RKO altered differentiation levels, masking the effect of drug compounds on the spheroids. Although the differentiation status of CRC cell line-generated spheroids has not been studied in depth before, it is known that 3D culture systems often change cell behaviour and cellular processes including differentiation (Edmondson et al., 2014). My results suggested a drive towards *DEFA5*-expressing Paneth cell lineage in SW480 with 3D culture alone, which had to be taken under consideration when interpreting results on experiments performed in 3D culture. GSK126 and DAPT treatment of SW480 spheroids downregulated default *DEFA5* expression shown in 3D culture conditions. I hypothesise that this could be due to Wnt signalling, where excessive push towards Wnt induction with both 3D culture conditions plus addition of GSK16 and DAPT, have led to the loss of cells' ability differentiate. Hyperactivation of Wnt is

known to perturb intestinal crypt plasticity by altering differentiation, proliferation and cause mis-positioning of differentiated cell types (Sansom et al., 2004).

Overall, the regulation of Wnt and Notch signalling pathways via drug compounds moderately affected secretory cell differentiation in the three CRC cell lines tested. However, due to the diversity in their default secretory cell gene expression and the limited differentiation potential of these CRC cell lines, although subtle changes were observed, a clean and uniform Paneth-like cell phenotype was not achieved with drug compound treatment.

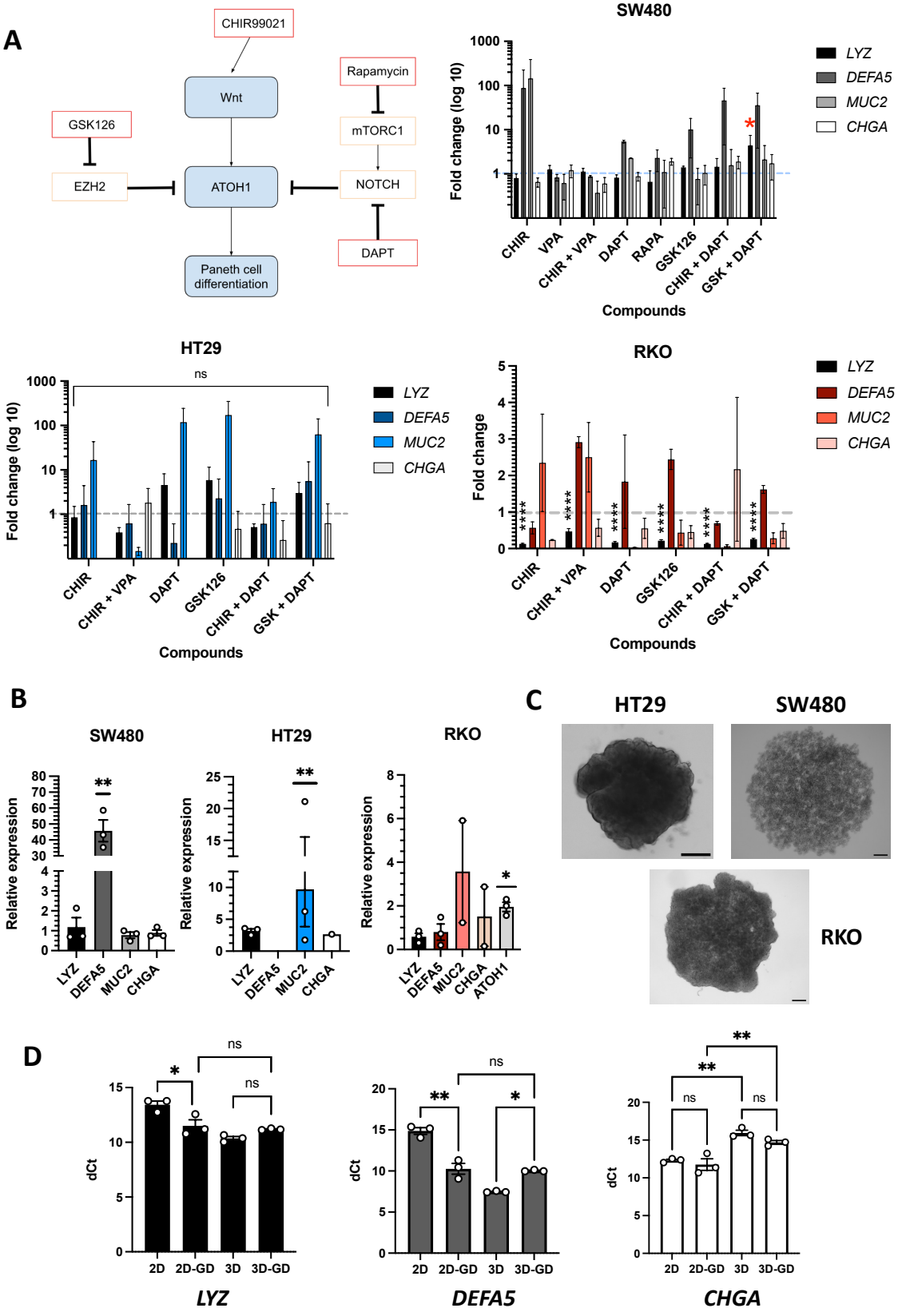

A
CHIR99021
Wnt
GSK126
EZH2
ATOH1
Rapamycin
mTORC1
NOTCH
DAPT
Paneth cell differentiation
SW480
Fold change (log 10)
LYZ
DEFA5
MUC2
CHGA
CHIR
VPA
CHIR + VPA
DAPT
RAPA
GSK126
CHIR + DAPT
GSK + DAPT
Compounds
HT29
ns
RKO
Fold change
B
SW480
HT29
RKO
Relative expression
ATOH1
C
HT29
SW480
RKO
D
dCt
2D
2D-GD
3D
3D-GD
LYZ
DEFA5
CHGA

Figure 3. Compound-induced Paneth cell differentiation in CRC cell lines cultured in 2D and 3D.

(A) (Top left) Schematic diagram of compounds (red box) targeting Paneth cell differentiation pathways. qPCR analyses showing relative *LYZ, DEFA5, MUC2* and *CHGA* expression in CHIR, VPA, CHIR + VPA, DAPT, RAPA, GSK126, CHIR + DAPT, GSK + DAPT treated cells compared to DMSO control for three CRC cells lines – SW480, HT29 and RKO. * P = 0.0269, **** P < 0.0001 using ordinary one-way ANOVA.

(B) qPCR analyses showing relative *LYZ, DEFA5, MUC2, CHGA* and *ATOH1* expression in HT29, SW480 and RKO spheroids compared to their 2D-cultured counterparts. * P = 0.0111, ** P < 0.01 using Student's t-test.

(C) Representative bright-field images of HT29 (top left), SW480 (top right) and RKO (bottom) spheroids cultured in 3D. Scale bars: 200 μm.

(D) qPCR dCt values (normalised to GAPDH) for *LYZ, DEFA5* and *CHGA* levels of SW480 cells cultured in 2D and 3D, treated with and without GSK126 and DAPT (GD). Lower dCt values represent higher mRNA levels. * P < 0.05, ** P < 0.01 using two-way ANOVA. All data are presented as the mean ± s.e.m

3.3 *ATOH1*-overexpression induces *DEFA5*+ Paneth cell signature and causes Jurkat cell infiltration

3.3.1 Introduction

ATOH1 is a transcription factor previously described to be involved in regulation of secretory cell differentiation in the small intestine (VanDussen & Samuelson, 2010), although distinct factors further down the secretory cell lineage defining goblet cell versus Paneth cell differentiation remain to be elucidated. Here, the direct overexpression of *ATOH1* was investigated for its ability to cause Paneth cell differentiation in CRC. mRNA levels of terminal secretory cell markers were measured through RT-PCR. SW480 cell line was chosen due to its baseline low expression levels of *ATOH1*, determined via RNA-sequencing (Barretina et al., 2012).

Furthermore, to evaluate immune response, a co-culture system with tumour spheroids and Jurkat cells was established. Jurkat cells are an immortalised human

T lymphocyte cell line obtained from an individual with T cell leukaemia (Schneider et al., 1977). The Jurkat line is commonly used to study activation of T cells, due to its ability of inducible secretion of cytokines and expression of early activation markers; processes regulated in the early activation of adaptive immune response (Alcamí et al., 1995; Clipstone & Crabtree, 1992). Jurkat cells can be artificially stimulated with Phorbol myristate acetate (PMA) and Ionomycin before usage in co-culture systems. PMA activates protein kinase C and ionomycin which is a calcium ionophore causes release of calcium signals. This method bypasses the T cell membrane receptor complex and cause intracellular signalling pathways stimulation, thus T cell activation and release of various cytokines, and is a common method to stimulate Jurkat cells before performing Jurkat cell activation assays (Abraham & Weiss, 2004a).

3.3.2 *ATOH1* overexpression induces *DEFA5* expression in SW480 2D and 3D spheroids

The introduction of *ATOH1* plasmid expression vector was performed using Lipofectamine, doxycycline was then added to induce the TetOn promoter and puromycin used for selection. Transfected cells successfully overexpressed *ATOH1* in SW480, confirmed by RT-qPCR. *ATOH1* overexpression (*ATOH1*+) caused a significant average 50-fold increase in mRNA levels of *DEFA5* (Fig 5A), reflecting the successful induction of Paneth cell gene expression in SW480. This elevated *DEFA5* expression in SW480 was sustained for up to 10 days post transfection, even following the drop of *ATOH1* levels back to base levels after day 5 (Fig 5B). Interestingly and coinciding with my *in-silico* analysis, the expression of *LYZ* did not follow *DEFA5* expression increase and was even observed to be slightly

downregulated (Fig 5A). Additional immunofluorescence staining confirmed the substantial increase in DEFA5 protein levels of SW480 *ATOH1*+ cells, with no clear change seen in LYZ protein levels (Fig 5C). This suggests that the expression of *DEFA5* and *LYZ* are not correlated *in vitro* in the context of CRC, supporting the heterogeneity of Paneth-like cell gene expression in CRC.

Following puromycin selection after *ATOH1* plasmid transfection, *ATOH1*+ cells were subsequently grown into 3D spheroids. SW480 *ATOH1*+ spheroids showed further 9-fold upregulation of *DEFA5* expression compared to non-transfected spheroids (Fig 5D). No morphological difference was observed between control and *ATOH1*+ SW480 spheroids and DAPI staining did not show any marked differences in the number of dead cells, although dead cells were concentrated in the core of both spheroids, likely due to the natural hypoxic environment of the spheroid core (Fig 5E). Furthermore, the sphericity index and area of spheroids were measured, and no changes were displayed between control and *ATOH1*+ spheroids (Fig 5F). As described earlier, wild-type SW480 spheroids already have high *DEFA5* expression, however I showed here that *ATOH1* overexpression pushed cells further driving more *DEFA5* expression compared to non-transfected SW480 spheroids, allowing them to be a tractable model to test the effects of Paneth cell differentiation. Of note, not all cells showed efficient transfection even after antibiotic selection as shown through immunofluorescence (Fig 5C), this adds an extra layer of heterogeneity within the spheroid, but also mimics what would happen *in vivo* as not all cells within the tumour would possess Paneth cell gene expression.

3.3.3 Jurkat cells as a model for T cell activation

An upregulation of early T cell activation markers *CD25*, *CD69*, *IL2* and *HLA-DR* expression was seen when PMA and ionomycin (PMA/I) were used to stimulate Jurkat cells. This was confirmed by RT-PCR (Fig 4A). CD25 seemed to be very poorly detected using flow cytometry (Fig 4B), albeit expression increased in a dose-dependent fashion. PD1 levels remained fairly similar for most PMA/I concentrations, but increased with 500 ng/mL PMA and 1 µg/mL ionomycin. CD69 expression was observed to be binary, with high expression even with low dose concentrations of PMA/I. As expected, the percentage of live cells markedly decreased with increasing dose concentration, thus an optimised drug concentration was used to overcome this. In terms of the duration of stimulation (Fig 4C), CD69 appeared to be the earliest marker, with drastic increase after 24 hours of stimulation. PD1 increased up until 48 hours but decreased again after 72 hours of stimulation. CD25 expression was low throughout 72 hour stimulation through flow cytometry detection, although upregulation of mRNA levels were observed through RT-PCR. Following these pilot experiments, PMA and Ionomycin at a dose of 50 ng/mL and 1 µg/mL respectively, were selected to stimulate Jurkat cells for 24 hours prior to co-culturing with tumour spheroids for a further 24 hours.

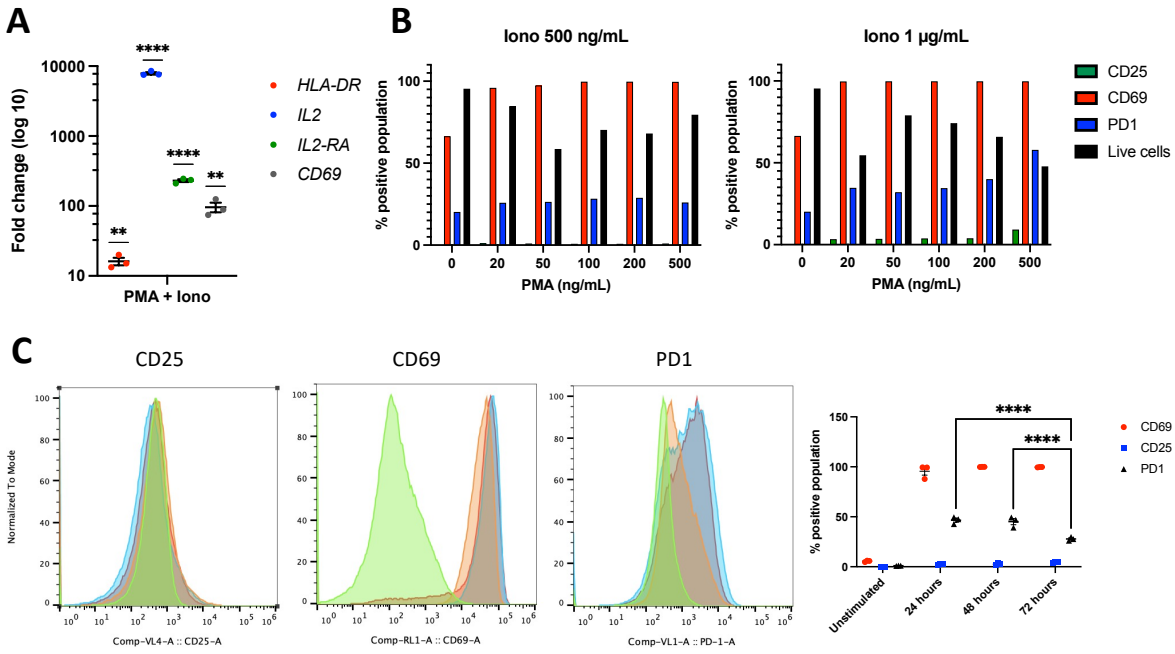


Figure 4. Jurkat cell is stimulated with PMA and Ionomycin to express early activation markers.

(A) qPCR analysis of *HLA-DR, IL2, IL2*-RA and *CD49* expression in Jurkat cells stimulated with PMA (50 ng/mL) and Ionomycin (1 µg/mL) for 24 hours. ** P < 0.01, **** P < 0.0001 using ordinary one-way ANOVA.

(B) Flow cytometric analyses showing percentage of CD25+, CD69+, PD1+ and live (determined by NEAR-IR staining) Jurkat cells after PMA/I stimulation for 24 hours at different doses.

(C) Flow cytometric analyses of Jurkat cells stimulated with PMA (50 ng/mL) and Ionomycin (1 µg/mL) at different time points.
(left) Histograms showing fluorescence intensity of CD25, CD69 and PD1 markers. Green – unstimulated; red – 24 hours; blue – 48 hours; orange – 72 hours.
(right) Quantification of CD25+, CD69+, PD1+ Jurkat cells at different time points.
**** P < 0.0001
All data are presented as the mean ± s.e.m

3.3.4 *ATOH1*-overexpression enhances Jurkat cell infiltration and IL2 secretion

To investigate how the induction of Paneth cell *DEFA5* expression affects tumour immunogenicity and immune cell migration, *ATOH1*+ spheroids were co-cultured with PMA/I-stimulated and unstimulated Jurkat cells and assays performed to explore Jurkat cell behaviour. First, following 24 hours of co-culture, Jurkat cells infiltrated the tumour spheroids, with stimulated Jurkat cells to a greater extent than unstimulated, as expected (Fig 5E). Strikingly, there was a significant increase in

the number of Jurkat cells within the *ATOH1*+ spheroids for both PMA/I-stimulated and unstimulated conditions compared to control spheroids, determined through fluorescent microscopy (Fig 5E,G).

Through flow cytometric analyses on Jurkat cell activation markers, there were significant differences in activation of Jurkat cells in co-culture compared to monoculture. CD25 and PD1 of stimulated Jurkat cells were significantly increased when co-cultured with spheroids; but PD1 and CD69 of unstimulated cells were decreased in co-culture compared to monoculture (Fig 5H). Since CD25 and PD1 represent early activation markers, this demonstrated that co-culturing with tumour spheroids alone caused an increase in activity of stimulated Jurkat cells. However, no marked differences in early activation markers CD25, CD69 and PD1 of Jurkat cells were seen when co-cultured with *ATOH1*+ spheroids as compared to controls (Fig 5H).

Jurkat cell activation is also commonly measured via secretion of Interleukin-2 (IL2). Jurkat cells are known to produce little IL2 in their resting state and upon stimulation this can be further increased (Weiss et al., 1984). Therefore, IL2 ELISA was performed on the media supernatant of control and *ATOH1*+ spheroids co-cultured with PMA/I-stimulated and unstimulated Jurkat cells. Results showed that external stimulation by PMA/I alone caused an increase in IL2 secretion of Jurkat cells in monoculture, as expected (Fig 5I). Co-culture of unstimulated Jurkat cells with tumour spheroids alone caused significant increase in IL2 secretion relative to monoculture, and these levels were also comparable to stimulated Jurkat cells co-cultured with spheroids (Fig 5I). There was a non-significant mean increase in IL2

concentration when unstimulated and stimulated Jurkat cells were co-cultured with *ATOH1*+ spheroids (Fig 5I). IL2 concentration was also measured in a 2D co-culture system in which SW480 cells were seeded in an adherent plate, hence default *DEFA5* expression in control SW480 cells are low, and Jurkat cells were added in suspension. Results indicated a non-significant mean increase in IL2 secretion in *ATOH1*+ cells co-cultured with stimulated Jurkat cells in 2D conditions compared to control (Fig 5J).

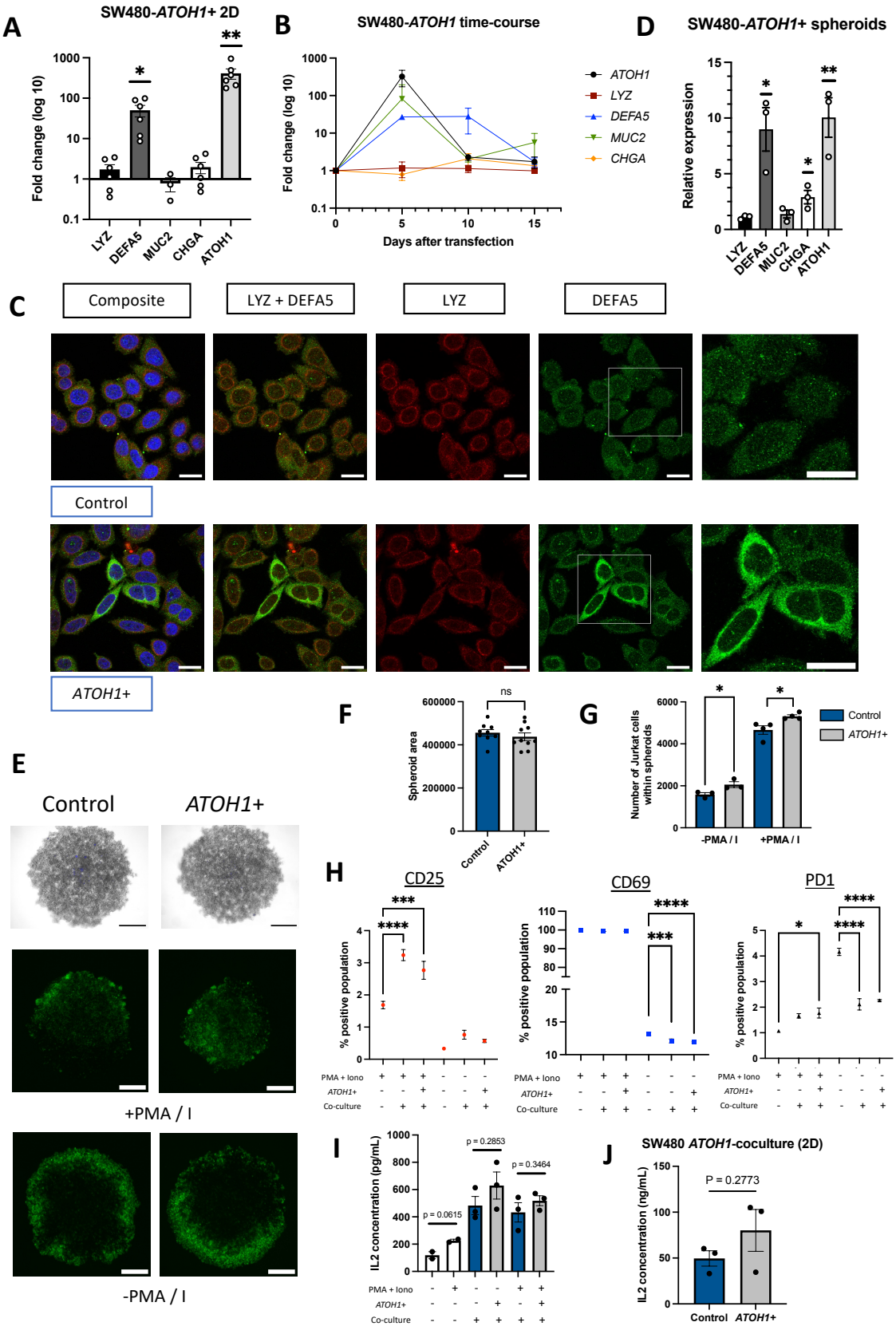

A
SW480-ATOH1+ 2D
Fold change (log 10)
LYZ
DEFA5
MUC2
CHGA
ATOH1
B
SW480-ATOH1 time-course
Fold change (log 10)
Days after transfection
ATOH1
LYZ
DEFA5
MUC2
CHGA
D
SW480-ATOH1+ spheroids
Relative expression
C
Composite
LYZ + DEFA5
LYZ
DEFA5
Control
ATOH1+
E
Control
ATOH1+
+PMA / I
-PMA / I
F
Spheroid area
ns
Control
ATOH1+
G
Number of Jurkat cells within spheroids
Control
ATOH1+
-PMA / I
+PMA / I
H
CD25
CD69
PD1
% positive population
PMA + Iono
ATOH1+
Co-culture
I
IL2 concentration (pg/mL)
p = 0.0615
p = 0.2853
p = 0.3464
J
SW480 ATOH1-coculture (2D)
IL2 concentration (ng/mL)
P = 0.2773
Control
ATOH1+

Figure 5. *ATOH1* overexpression on SW480 cells induces *DEFA5*+ Paneth cell differentiation, Jurkat cell infiltration and IL2 secretion.

(A) qPCR relative expression of *LYZ, DEFA5, MUC2, CHGA* and *ATOH1* of *ATOH1*-overexpressed SW480 cells in 2D culture. *P< 0.05, **P< 0.01 using ordinary one-way ANOVA.

(B) qPCR analysis showing expression levels of *LYZ, DEFA5, MUC2, CHGA* and *ATOH1* of *ATOH1*-overexpressed SW480 cells every 5 days post-transfection relative to non-transfected cells grown in the same conditions.

(C) Representative immunofluorescence images of SW480 control and *ATOH1*-overexpressing cells. DAPI (blue), LYZ (red) and DEFA5 (green). Scale bar: 20 μm.

(D) qPCR relative expression of *LYZ, DEFA5, MUC2, CHGA* and *ATOH1* of *ATOH1*-overexpressed SW480 spheroids, compared to non-transfected spheroids grown in the same 3D conditions.
*P< 0.05, **P< 0.01 using ordinary one-way ANOVA.

(E) (top) Representative bright-field of control and *ATOH1*-overexpressing SW480 spheroids stained with DAPI. (bottom) GFP+ channel images showing SW480 control and *ATOH1*-overexpressing spheroids co-cultured with for 24 hours Jurkat cells. GFP represents Jurkat cells, unstimulated or stimulated with PMA (50 ng/mL) and Ionomycin (1 μg/mL) for 24 hours. Scale bars: 500 μm.

(F) Sphericity index of control versus *ATOH1*+ SW480 spheroids. N.S. using Student's t-test.

(G) Quantification of GFP+ Jurkat cells within the spheroids. * P < 0.05 using Student's t-test.

(H) Flow cytometry analysis of Jurkat cell activation markers CD69, CD25 and PD1, defined as percentage positive population of stimulated or unstimulated Jurkat cell in monoculture, or co-cultured with control and *ATOH1*-overexpressing spheroids. *P< 0.05, ****P< 0.0001 using 2way ANOVA.

(I) ELISA-IL2 secretion concentration (pg/mL) of media supernatant of stimulated or unstimulated Jurkat cell in monoculture, or co-cultured with control and *ATOH1*-overexpressing spheroids. Using Student's t-test.

(J) ELISA-IL2 secretion concentration (ng/mL) of media supernatant of stimulated Jurkat cell co-cultured with control and *ATOH1*+ cells in cultured in 2D. Using Student's t-test. All data are presented as the mean ± s.e.m

3.3.5 *ATOH1* overexpression in HT29 causes *DEFA5* level increase and inhibits spheroid formation

Next, I sought to validate my findings in a different cell line – HT29, which is also MSS. Similarly, *ATOH1* overexpression was performed on HT29 cells and a substantial average 150-fold increase in *DEFA5* expression was achieved in 2D culture conditions (Fig 6A). *MUC2* expression was also increased with *ATOH1* overexpression in HT29, however the fold change (7-fold) was relatively low compared to *DEFA5*. There was also a significant decrease in *LYZ* expression observed, again emphasising the differential regulation of *LYZ* and *DEFA5* transcriptionally in CRC (Fig 6A). Interestingly, when HT29 *ATOH1*+ cells were

subsequently grown into 3D spheroids, a distinct morphology compared to the non-transfected control spheroids was observed. *ATOH1* overexpression was still retained in 3D culture (Fig 6B), however high raw RT-PCR Ct values revealed downregulation of *DEFA5* expression in both control and transfected spheroids. It appeared that *ATOH1* overexpression inhibited the formation of fully intact and cystic HT29 spheroid structures as compared to wild type (Fig 6C). Although the inner core of the *ATOH1*+ spheroids contained more dense cell aggregates and hints of spheroid formation, many cells on the outer layer failed to come close together for spheroid formation. This was demonstrated through DAPI staining of live spheroids, in which most of the single cells present around the spheroid appeared to be dead, in contrast to control spheroids that only contained a few dead cells within the core of the spheroids (Fig 6C), similar to SW480 spheroids. I hypothesise that the combination of 3D culturing and forced expression of *ATOH1* may have over-differentiated the cells and suppressed subsequent proliferation from more clonogenic populations, preventing formation into spheroids.

HT29 *ATOH1*+ spheroids were likewise co-cultured with unstimulated and PMA/I-stimulated Jurkat cells. A subtle increase in Jurkat cell attraction was seen, observed through the increase in GFP intensity around *ATOH1*+ spheroids (Fig 6D). Additionally, similar to observations seen in SW480, there was a mean increase in IL2 concentration when Jurkat cells were co-cultured with *ATOH1*+ spheroids (Fig 6E), although not statistically significant.

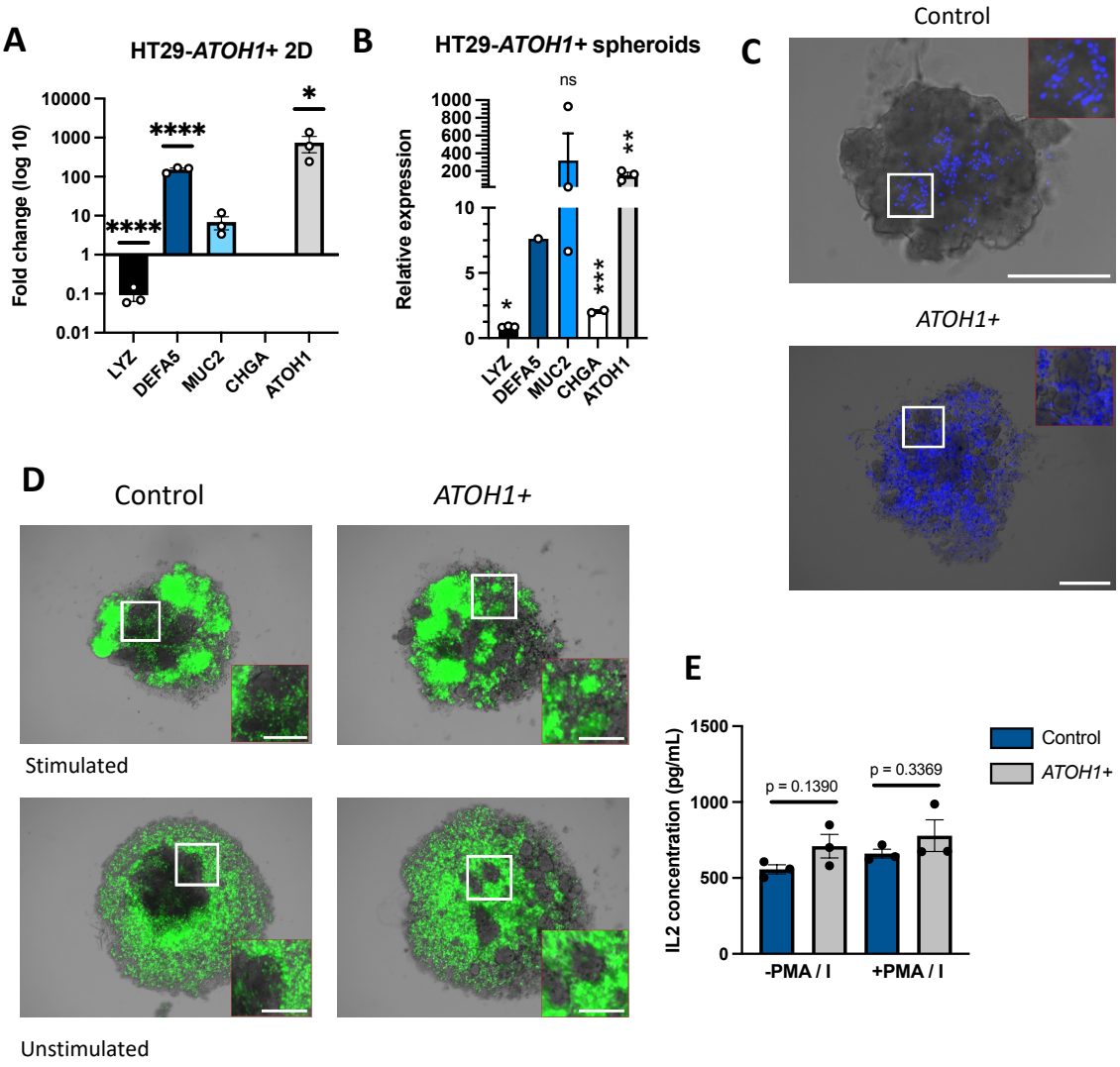


Figure 6. *ATOH1* overexpression on HT29 cells induces *DEFA5* expression but hinders spheroid formation.

(A) qPCR relative expression of *LYZ, DEFA5, MUC2, CHGA* and *ATOH1* of *ATOH1*-overexpressed HT29 cells in 2D culture. *P< 0.05, ****P< 0.0001 using ordinary one-way ANOVA.

(B) qPCR relative expression of *LYZ, DEFA5, MUC2, CHGA* and *ATOH1* of *ATOH1*-overexpressed SW480 spheroids, compared to non-transfected spheroids grown in the same conditions. *P< 0.05, **P< 0.01, *** P < 0.001 using ordinary one-way ANOVA.

(C) Representative bright-field images of HT29 control and *ATOH1*-overexpressing spheroids. DAPI (blue). Scale bars: 400 µm.

(D) Microscopy images showing HT29 control and *ATOH1*-overexpressing spheroids after co-culture with Jurkat cells for 24 hours. GFP+ cells represent Jurkat cells, unstimulated (bottom) or stimulated (top) with PMA (50 ng/mL) and Ionomycin (1 µg/mL) for 24 hours. Scale bars: 400 µm

(E) ELISA-IL2 secretion concentration (pg/mL) of media supernatant of stimulated or unstimulated Jurkat cells co-cultured with control and *ATOH1*-overexpressing spheroids. Using Student's t-test.

All data are presented as the mean ± s.e.m

3.3.6 Discussion

To summarise, direct *ATOH1* overexpression was able to induce *DEFA5*-expressing Paneth-like cell differentiation in SW480 and HT29 cell lines. Induced *DEFA5* expression in Paneth-like cells appeared to play a role in the attraction and hence infiltration of Jurkat cells into the tumour spheroids, which may be beneficial in a cancer context as migration of T cells towards the tumour is clearly essential for effective host-tumour cell interactions. Furthermore, IL2 is an immune modulatory cytokine predominantly secreted by activated T cells and is important for the proliferation of cytotoxic T cells, differentiation of B cells, NK cells, monocytes and macrophages (Boyman & Sprent, 2012). In my results, *ATOH1* overexpression which caused high *DEFA5* expression in HT29 and SW480 led to a non-significant mean increase in IL2 release from Jurkat cells, further validation needs to be performed in order to determine whether this trend is true. HT29 and SW480 are both MSS cancer cell lines. In the clinical setting MSS cancers do not respond well or predictably to immunotherapy and are often described as 'immunogenically cold' due to limited infiltration of T lymphocytes. Here, I showed that Paneth cell differentiation with high *DEFA5* expression potentially enhances immune response against the tumour via increased infiltration of immune cells.

Jurkat cell activation was also measured via flow cytometric analyses of known early activation markers CD25, CD69 and PD1. When cultured alone, PD1 expression of PMA/I-stimulated Jurkat cells dropped after 72 hours, likely due to the lack of tumour interaction. Interestingly, PD1 expression in unstimulated Jurkat cells was decreased during co-culture with SW480 spheroids. Co-culture with tumour spheroids has the ability to affect Jurkat cell activity (Zheng et al., 2019). It is

possible that since SW480 moderately expresses PD-L1, a ligand for PD1 (Xu et al., 2021), PD1 on unstimulated Jurkat cells interacts with PDL1 and therefore internal feedback mechanisms occur to reduce activity of Jurkat cells and hence PD1 and CD69 activation markers are downregulated. When Jurkat cells are stimulated with PMA/I, they are possibly able to escape this due to high intrinsic calcium signalling driving activation cues.

However, no significant differences were seen in activation markers of Jurkat cells in *ATOH+* spheroids compared to control spheroids. Although I showed that Jurkat cell activation was altered via co-culture with spheroids, several underlying limitations to this co-culture system remain. Jurkat cells are clones of T lymphocytes therefore only have one T cell receptor (TCR), which makes it difficult to recognise the limited antigens present in CRC cell lines which are also clonal. PMA and Ionomycin stimulation bypasses the T cell membrane receptor complex, therefore it could be that a different stimulant is required for the increased affinity of TCRs to exhibit downstream immune regulation. Considering the limited TCR affinity of Jurkat cells for tumour antigens, I therefore hypothesise that *DEFA5* overexpression alone was not sufficient to cause visible changes in activation markers presented on the surface of Jurkat cells.

3.4 SATB2-KO in SW480 induces *DEFA5* expression and Jurkat cell IL2 increase

3.4.1 Introduction

The importance of mutations in chromatin modifying genes and the role of aberrant regulation of chromatin modification in CRC have been increasingly recognised. (Sottoriva et al., 2021) recently identified recurrent somatic missense mutations in chromatin modifier genes in MSS CRC, particularly in the lysine demethylases (KDM), lysine acetyltransferases (KAT), lysine methyltransferases (KMT) and SWI/SNF families. These mutations pointed at important roles in immune remodulation and reactivation of developmental gene programmes. Several papers have also previously described the importance of chromatin dynamics in the regulation of secretory cell fate. Importantly, specific chromatin modifiers such as EP300, HDAC1/2, KDM1A, which are amongst the list of mutated chromatin modifier in (Sottoriva et al., 2021), have demonstrated specific roles in modulating Paneth cell numbers in the small intestine (Hiramatsu et al., 2019; Ostrop et al., 2021; Turgeon et al., 2013; Zwiggelaar et al., 2020). I therefore sought to investigate whether modifications of a specific chromatin modifier gene using CRISPR-cas9 knockout techniques was able to induce a Paneth cell phenotype in CRC, and whether this had an effect on Jurkat cell activity.

3.4.2 SATB2 knockout induces *DEFA5*+ Paneth cell differentiation

To decide which gene to target, TCGA gene expression data of chromatin modifier genes were analysed, and co-expression with secretory cell differentiation markers plotted (Fig 7A). Results revealed that SATB Homeobox 2 (*SATB2*) was the most

significantly and negatively correlated with Paneth cell marker *LYZ* (Spearman's correlation = -0.488; q-value = 6.17E-30). SATB2 is a DNA binding protein that specifically binds to nuclear matrix attachment regions and is involved in transcriptional regulation and chromatin remodelling. Recently, (Gu et al., 2021) demonstrated that loss of SATB2 transforms colonic epithelium into ileum-like tissue in mice and in human colonic organoids. With this, there was an increase in Paneth cells. I therefore tested whether SATB2 plays a role in Paneth cell differentiation in CRC.

CRISPR-cas9 electroporation of sgRNA targeting Exon 4 of *SATB2* was performed to knockout SATB2 in SW480 cell lines that had already been mCherry labelled. A successful knockout was attained and confirmed by Sanger sequencing. Single-cell cloning was performed to obtain a clonal knockout population. This clonal population contained a single nucleotide deletion at the site of guideRNA cut-site (Fig 7C) that resulted in a frameshift and therefore depletion of SATB2 protein, which was validated by Western blot (Fig 7B). SATB2 knockout (KO) in SW480 cell line caused upregulation of Paneth cell gene expression, however surprisingly, clonal SATB2-KO cell lines grown in 2D culture exhibit 12-fold elevated expression of *DEFA5* rather than *LYZ* (Fig 7D), although this increase was not as great as that seen in *ATOH1* overexpressing cells. Even though there was negative correlation between *SATB2* and *DEFA5* expression (Spearman's correlation = - 0.03) described in TCGA data, this was not statistically significant (q value = 0.69). It was therefore surprising to observe *DEFA5* increased expression rather than *LYZ* through RT-PCR. The difference in protein levels was also confirmed by immunofluorescence, showing an increase in DEFA5 protein but not LYZ in SATB2-

KO cells (Fig 7E). The SATB2-knockout line was also cultured into 3D spheroids. Again, due to the differentiation push of high *DEFA5* expression during 3D culture, the effect of SATB2-knockout on *DEFA5* expression was reduced, with only 2-fold difference compared to control spheroids (Fig 7D). SATB2-KO cells looked morphologically similar to control cells in both 2D and 3D culture.

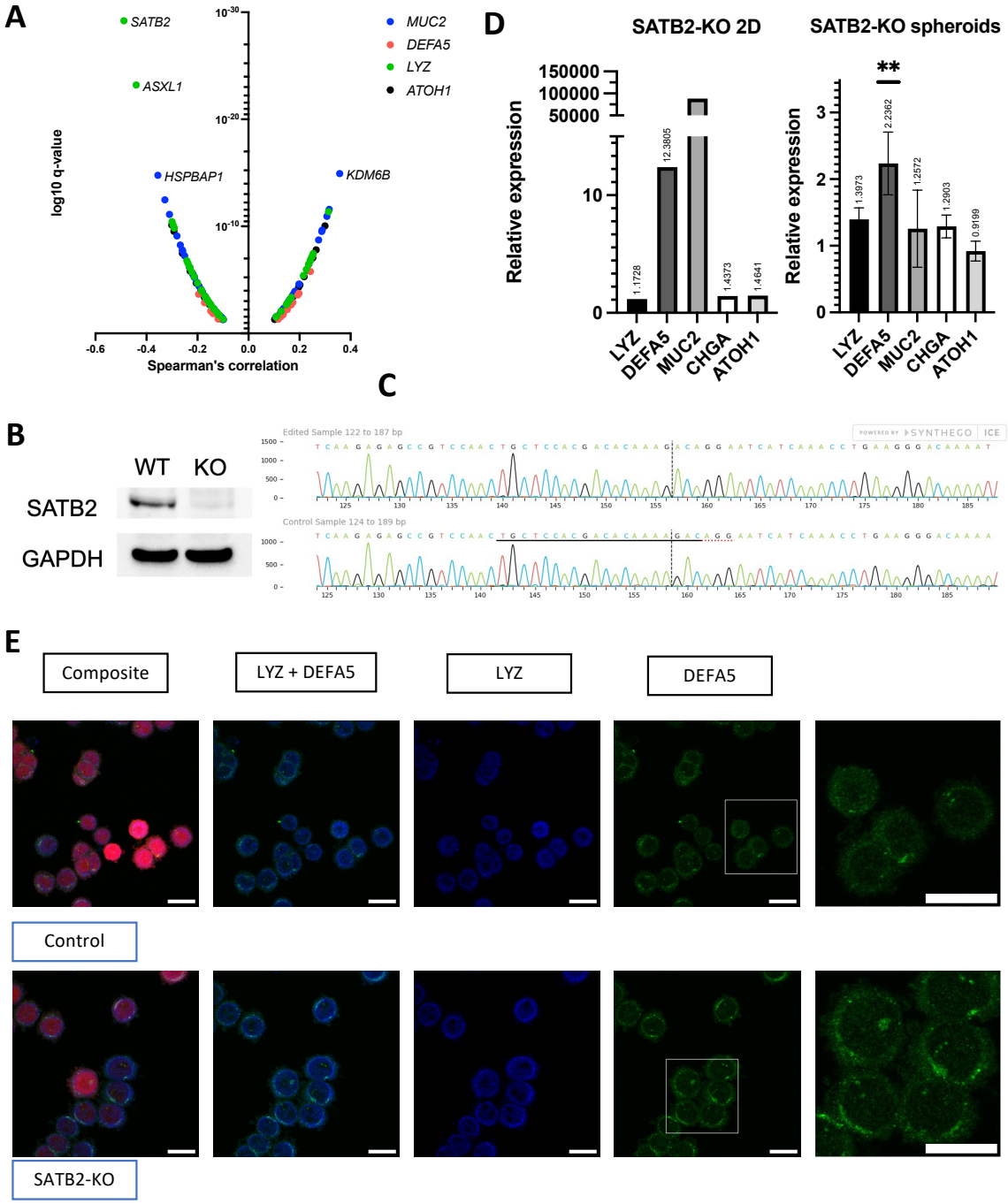


Figure 7. SATB2 CRISPR-knockout on SW480 cells induces *DEFA5*+ Paneth cell differentiation.

(A) Volcano plot showing Spearman's correlation of expression of chromatin modifier genes (points) with common missense mutations in microsatellite stable CRC and differentiation markers *MUC2, DEFA5, LYZ* and *ATOH1*.
(B) Western blot showing SATB2 protein levels in SW480 wildtype (WT) and knockout (KO).
(C) Sanger sequence of control SW480 versus SATB2-KO line showing a single-nucleotide deletion. Analysis produced via Synthego ICE.
(D) qPCR relative expression of *LYZ, DEFA5, MUC2, CHGA* and *ATOH1* of SATB2-KO cells compared to control cells cultured in 2D (left) and as 3D spheroids (right). *P< 0.05, **P< 0.01 using ordinary one-way ANOVA. Data presented as the mean ± s.e.m
(E) Representative immunofluorescence images of SW480 control and SATB2-KO cells. mCherry-labelled cells (red), LYZ (blue) and DEFA5 (green). Scale bar: 20 μm.

3.4.3 SATB2-KO increases Jurkat cell IL2 secretion

SATB2-KO spheroids were also cocultured with PMA/I-stimulated and unstimulated Jurkat cells. Similar to *ATOH1*+ spheroids, results did not show significant changes of CD25, CD69 nor PD1 on the surface of Jurkat cells through flow cytometry (Fig 8C). Using fluorescence microscopy, an increase in Jurkat infiltration into the SATB2-KO spheroid compared to control was seen (Fig 8A). Stimulated Jurkat cells clumped together surrounding the spheroids, mimicking T cell clumping during activation. However, the area of SATB2-KO spheroids was significantly larger compared to control spheroids, thus there was no observed difference in the number of stimulated Jurkat cells infiltrating within the SATB2-KO spheroids compared to control spheroids once size of spheroid was used for normalisation (Fig 8B).

IL2 secretion of Jurkat cells was also measured in co-culture and monoculture. Co-culture alone caused a significant increase in IL2 concentration compared to mono-culture. Again, unstimulated Jurkat cells also secreted IL2 to a level comparable to that of stimulated Jurkat cells, when in co-culture with tumour spheroids. However, no differences were seen in IL2 concentration for control versus SATB2-KO co-

cultures in 3D (Fig 8D). This result could be explained by the push towards increased *DEFA5* expression in 3D culture alone. To overcome the marked increase in *DEFA5* expression in 3D culture, a 2D coculture system of SATB2-KO cells and Jurkat cells was also performed. ELISA of co-culture supernatant suggested a non-significant mean increase in IL2 concentration upon Jurkat cell co-culture with SATB2-KO cells (Fig 8D).

3.4.4 Discussion

I demonstrated here that loss of SATB2 was able to cause Paneth cell differentiation in a CRC model. However, a specific change in chromatin modification was not tested for, so alternative mechanisms for this change in *DEFA5* expression could theoretically be possible. Particularly, further investigation is required to reveal the reason for specific *DEFA5* but not *LYZ* overexpression with SATB2-KO. This is crucial as it may reveal chromatin modification as a mechanism specifying differential expression of these Paneth cell-specific antimicrobial peptides. Additionally, SATB2 is a chromatin modifier with pleiotropic functions, therefore I cannot conclude that the immune effects shown here is exclusively due to the increase in Paneth cell gene expression. Nevertheless, it appeared that loss of SATB2, a gene frequently mutated in CRC, caused an increase in *DEFA5*+ Paneth cell differentiation in the SW480 MSS cancer cell line and when co-cultured with Jurkat cells, led to a reproducible albeit non-significant trend in increase IL2 secretion.

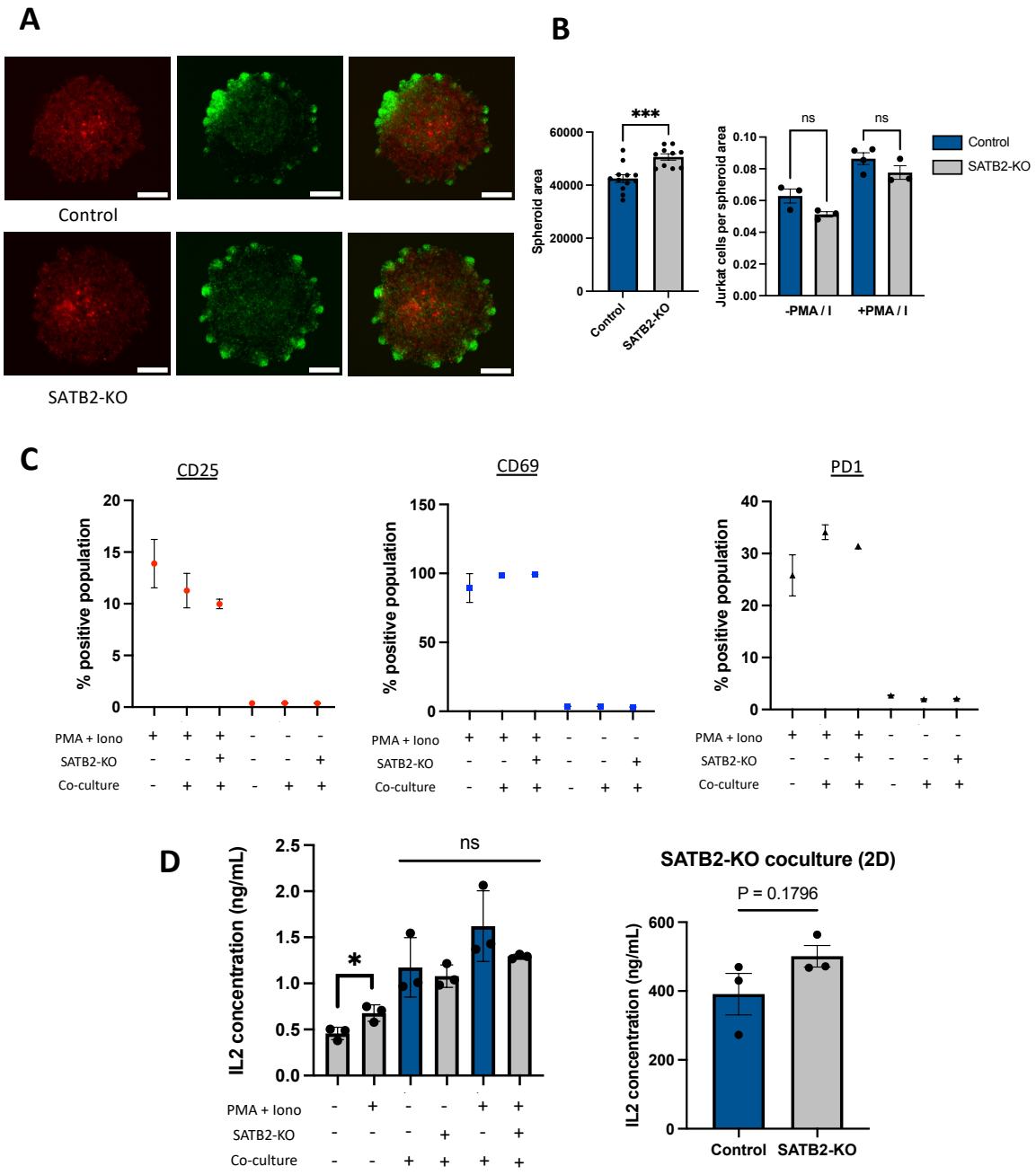


Figure 8. Co-culture with SATB2-KO cells causes increase in Jurkat cell IL2 secretion.

(A) Microscopy images showing SW480 control (top row) and SATB2-KO spheroids (bottom row) after 24 hours co-culture with Jurkat cells stimulated with PMA (50 ng/mL) and Ionomycin (1 µg/mL) for 24 hours. Red represent SW480 spheroids. GFP+ cells represent Jurkat cells. Scale bars: 500 µm

(B) (left) Sphericity index of control versus SATB2-KO SW480 spheroids. *** $P < 0.001$ using Student's t-test. (right) Quantification of GFP+ Jurkat cells within the spheroids per spheroid area.

(C) Flow cytometry analysis of Jurkat cell activation markers CD69, CD25 and PD1 defined as percentage positive population of stimulated or unstimulated Jurkat cell in monoculture, or co-cultured with control and SATB2-KO spheroids. N.S. using 2way ANOVA.

(D) ELISA-IL2 secretion concentration (ng/mL) of media supernatant of stimulated or unstimulated Jurkat cell in monoculture, or co-cultured with control and SATB2-KO cells in 3D spheroids (left) and 2D (right). Using Student's t-test.

4 Discussion

The majority of patients with MSS CRC suffer from poor efficacy of immunotherapy, and therefore conventional surgery, chemotherapy, anti-epithelial growth factor receptor and anti-angiogenesis treatments remain the only options in advanced disease. (Le et al., 2015) reported little to no immune-related objective response rate following anti-PD1 treatment in MMR-proficient cancers. Sadly, MSS tumours represent the majority of CRC patients, therefore given the striking results seen in MMR-deficient tumours there is an urgent imperative to find ways to enhance immune response against these tumours. A high LN yield during surgical resection of the CRC tumour is associated with improved survival. This increased LN yield is likely driven by enhanced immune response in the primary tumour, making lymph nodes more apparent (Lal et al., 2022). Yet, underlying genetic or epigenetic perturbations within the tumour to cause this increase in LN yield were not found to be deterministic.

It was exciting however to find that these high LN yield tumours have significant enrichment in a Paneth cell gene signature compared to the low LN yield group. Paneth cells in the small intestine play a functional role of immune modulation and regulation of the intestinal microbiota, and secretion of antimicrobial peptides and enzymes including lysozyme and alpha-defensins directly contribute to the innate immune system in destroying pathogens. It is however unclear whether Paneth-like cells in the colon and particularly in CRC, carry out similar functions. In this study, I found that although the expression of antimicrobial peptides *LYZ* and *DEFA5* were present in the normal colon, representing Paneth-like cells and Paneth cell gene

expression in the large intestine as previously described, the proteins expression was poorly correlated, unlike in Paneth cell populations of the small intestine. Importantly, the inverse correlation of *LYZ* and *DEFA5* expression seemed to be further amplified in CRC. This underlined vital information of the differential regulation of expression and possibly function of these Paneth cell-specific peptides in colonic tumours. Previously, (Ito et al., 2012) demonstrated that recombinant DEFA6 is able to cause chemotaxis of immature dendritic cells. On the other hand, (Grigat et al., 2007) showed that DEFA5 is a potent chemotaxin for the mobilisation of macrophages but not dendritic cells. Therefore, although there are structural conservations between these antimicrobial peptides that allow immune cell interactions, their sequence variability may also result in distinct immune system crosstalk and modulation. With that said, I hypothesise that the expression of *LYZ* versus *DEFA5* in CRC tumours might potentially have a differential effect on host immune response. It was therefore crucial to investigate the distinct functions of differential Paneth cell gene expression on immune response in CRC.

Paneth cells are usually absent/rare in the colon, where colorectal cancer develops, however Paneth cell metaplasia has been associated with diseased individuals including those with colorectal cancer and inflammatory bowel disease. In spite of that, prior studies have failed to evaluate the specific role of Paneth cells in CRC. A previous study (Pflügler et al., 2020) suggested that *LYZ*-specific Paneth cells were able to cause immune escape in CRC. Importantly, my GSEA results also showed that *LYZ*-expressing tumours were associated with low interferon gamma, interferon alpha and inflammatory response, however the opposite was observed with high *DEFA5*-expressing tumours, which showed enriched interferon gamma and alpha

responses. I therefore hypothesised that specific *DEFA5*-expressing Paneth-like cells in CRC are able to enhance the host-tumour immune response.

The first aim of the project was therefore to establish methods to induce the formation of Paneth-like cells in CRC models. *ATOH1* overexpression and SATB2-KO were able to achieve *DEFA5*+ overexpression in SW480 and HT29, and SW480 cell lines, respectively, reflecting the induction of Paneth-like cell differentiation with specific DEFA5 secretion. In both cases, RT-PCR and immunofluorescence revealed that *DEFA5* and *LYZ* expression was not mirrored and *ATOH1* overexpression only increased *DEFA5* expression and not *LYZ*, which allowed us to test the specific role of *DEFA5* expression in the context of CRC. Detailing the mechanisms of how *DEFA5* and *LYZ* expression is regulated in CRC clearly requires further investigation.

Considering the role of SATB2 as a chromatin modifier, chromatin changes might play a role in specifying peptide expression. It is also possible that other transcription factors apart from ATOH1 are involved in directing terminal secretory cell fate. A previous study (Leow et al., 2004) also presented that upregulation of *ATOH1* in HT29 caused increased number of goblet cells, which is the main secretory cell type that is commonly found in the colon. My results here indicated that overexpression of *ATOH1* increased *DEFA5*+ Paneth cell differentiation expression to a greater extent than goblet cell differentiation in both HT29 and SW480 cell lines.

Using these specific *DEFA5*+ Paneth cell differentiated CRC models, I was able to test the specific role of DEFA5 on T-cell activation and infiltration. The increased Paneth cell peptide DEFA5 generated in CRC spheroids prompted a substantially

greater influx of Jurkat cells into the spheroids during co-culture compared to control spheroids. This observation coincided with our initial multiomic *in silico* analysis in which there was a greater enrichment of T cells and B cells around tumours with a high Paneth cell signature (Lal et al., 2022). This also agrees with a study (Grigat et al., 2007) that demonstrated the ability of DEFA5 to attract naïve as well as memory T lymphocytes. Of note, activation markers CD69, CD25 and PD1 expressed by these Jurkat cells were not significantly changed when co-cultured with DEFA5-high spheroids compared to control in my study. This possibly demonstrates that although these immune cells are being attracted to the tumour, they might not be activated by the cellular changes associated with increased *DEFA5* expression. Nonetheless, an infiltration of T cells represents benefits to tumour destruction and often presents better prognosis (Naito et al., 1998; Prall et al., 2004). An increased number of T cells surrounding and infiltrating the tumour increases the chances of tumour cell recognition and further downstream activation. T cells have roles in direct tumour-killing and also secretion of cytokines to modulate the immune system (Raskov et al., 2020). Although precise mechanisms of how DEFA5 interacts with immune cells is yet to be known, (Lisitsyn et al., 2012) proposed binding of DEFA5 to an unidentified G-protein coupled receptor on macrophages and T cells induces their chemotaxis and subsequent proliferation. My data suggests a potentially similar process occurring in a tumour context where increased *DEFA5* expression enhances the interaction between epithelial cells and immune cells, to overcome the insufficient antigen presentation in MSS CRCs, since SW480 and HT29 are MSS cell lines.

My analyses also showed a non-significant trend towards an increase in Jurkat cell IL2 secretion upon co-culturing with *ATOH1*+ and SATB2-KO cells. Recombinant IL2 was the first immunotherapy to be approved by FDA (Rosenberg, 2014). IL2 has also been known to have anti-colorectal cancer tumour growth properties (Y. Wang et al., 2016). IL2 secretion represents elevated activation of Jurkat cells that is usually mediated via T cell receptor recognition. Ideally, *DEFA5* expression could potentially have the ability to improve T cell receptor recognition and binding, increasing cytokine production of immune cells. In this case, differentiation therapy could have an additive effect on IL2-mediated immunotherapy, and potentially be used to overcome limitations of IL2 therapy such as its short life-span and high-dose toxicity. Previous studies also reported that addition of DEFA5 peptides to colonic intestinal epithelial cells was able to induce upregulation of IL8 secretion (de Leeuw et al., 2007; Ishikawa et al., 2010). IL8 is responsible for attracting neutrophils to site of inflammation (Bickel, 1993). In my model however, the increase in IL2 secretion from Jurkat cells following co-culture with *ATOH1*-overexpressing and SATB2-KO spheroids was not statistically significant, therefore a different model and further experiments for validating the effect of Paneth cell differentiation on immune cell cytokine production should be established.

ATOH1 is a tumour suppressor gene and is downregulated in 70% of CRC (Kazanjian & Shroyer, 2011). Forced expression of *ATOH1* in HT29 cell lines inhibited their proliferation (Leow et al., 2004). Similarly in my project, *ATOH1* overexpressing HT29 cells displayed reduced formation of intact spheroids in 3D suspension culture. In light of this, I propose that the rescue of *ATOH1* expression in CRC may not only restrict tumour growth, but also potentially drive tumours

towards a more secretory cell or Paneth-like cell differentiated state, which I showed here might be involved in stimulating immune cell infiltration and cytokine secretion. Furthermore, recently, SATB2 has gained increasing attention as a marker for colorectal differentiation (Eberhard et al., 2012; Sottoriva et al., 2021). Crucially, (Brennan et al., 2019) stated that SATB2 presented strong relations and conferred a master regulator of inflammation in CRC. SATB2-low tumours were also found to be enriched in CMS1 subtype (Brennan et al., 2019), which represent majority of MSI-H tumours with enriched infiltration of immune cells. Here I present further insight and speculate the role of Paneth cell differentiation as the mediating factor of SATB2 inflammatory regulation in the tumour. This is crucial as if one can show that SATB2 mutations in CRC are able to enhance tumour immunogenicity, through the upregulation of Paneth cell gene markers, then this could potentially be predictive of immunotherapy responses.

Different compounds targeting known Paneth cell differentiation pathways were also investigated for their ability to establish a Paneth-like cell phenotype in CRC. Although the majority of drug combinations showed no marked differences on terminal differentiation markers in CRC cell lines, EZH2 inhibitor GSK126 and DAPT combination marginally increased Paneth cell differentiation in SW480 cells. This demonstrates that the upregulation of Wnt and downregulation of Notch signalling with these drugs may have the ability to differentiate some MSS cancers towards a Paneth cell lineage. The potential ability for EZH2 inhibitors to improve efficacy of immune therapies has previously been described (Li et al., 2021). Combinatorial therapy of GSK126 and anti-PD1, enhanced MHC class I antigen presentation and T-cell mediated killing with reduced tumour growth in head and neck squamous cell

carcinoma (Zhou et al., 2020). Here I suggest that since treatment with GSK126 and DAPT caused moderate Paneth cell differentiation in a MSS cancer cell line, this could potentially aid immunotherapy efficacies that are administered in combination. Of note, some cell lines are known to have restricted differentiation potential, and the optimum dose and time for drug treatments on cell lines cultured in 2D and 3D were not investigated in this study, and this requires further exploration. With more time, the efficient dose and time can be determined for drugs to allow sufficient secretory cell differentiation within the tumour to exhibit an enhanced immune response. Potentially, differentiation therapy such as GSK126 in combination with DAPT could improve responses to immunotherapy, especially in MSS cancers with typical poor responses.

I showed here that the presence of Paneth cells or Paneth cell-specific peptide expression may be beneficial to CRC patients. Although some research has been done to look at the role of Paneth cells in CRC, based on literature review, Paneth cell presence seem to have negative impact on early CRC tumourigenesis, due to their Wnt-providing role and source of intestinal stem cell niche (X. Liang et al., 2022; Sato et al., 2011). An elevated number of Paneth cells is associated with Notch and Wnt activation and poor prognosis (López-Arribillaga et al., 2021), although with contradictory reports also described (Mahon et al., 2016). Importantly, a recent single-cell paper (Burclaff et al., 2022a) showed that normal healthy human Paneth cells in the small intestine differ from those in mice in that they do not possess any Wnt ligand expression and thus might not contribute to the stem cell niche compartment. *ATOH1* knockout in mice showed no difference in the stem cell niche compared to control; loss of Paneth cells did not perturb architecture nor beta-

catenin signalling (Durand et al., 2012b). Hence, initiation of tumourigenesis and progression to carcinoma can be argued to be Paneth cell independent. In our paper, LN yield and immune response association occurs regardless of MSS or MSI-H status and CMS subtype, hence the presence of Paneth cells could be the underlying reason behind enrichment in immune response and thus enhanced LN yield and survival. The induction of Paneth cell differentiation in tumours could therefore be of clinical interest.

Limitations:

Overall, I showed that *ATOH1* overexpression and SATB2-KO were able to create a Paneth-like cell phenotype in the context of CRC models and used as models to test for effects on immune response. There are however some limitations to the co-culture system I have established and therefore limitations to the potential findings my results can provide. First, SW480 cells (which is the main cell line chosen to perform experiments) showed drastic changes in differentiation status when cultured in 3D, with very high induction of *DEFA5* expression. Therefore, the large increase in *DEFA5* expression achieved through *ATOH1* overexpression and SATB2-KO in 2D culture was substantially reduced in spheroid culture conditions, which might have affected subsequent results. However, experimental conditions carried out in 2D cells were also co-cultured with Jurkat cells in 2D, and a reproducible immune phenotype was observed. Howbeit 2D co-culture systems do not enforce direct cell-to-cell interactions, which potentially limits the effect on immune response. Additionally, all 3 cell lines – HT29, SW480 and RKO also had different and limited differentiation potential and growing these CRC cell lines in 3D environment presented further heterogeneity, therefore the Paneth cell phenotype

was unable to be replicated and reproduced in each cell line. This made comparison of immune response measurements difficult.

Further, Jurkat cells were incorporated into the spheroid co-culture system and chosen as a mimic of T cell activation to test for immune effects due to its robust history as a model in the discoveries of T cell receptor (TCR) stimulation (Abraham & Weiss, 2004b). Jurkat cell immortality also allowed preliminary experiments to be more conveniently conducted. However, since the immortalised Jurkat cell line is clonal, this demonstrates that TCRs presented on the Jurkat cells are only able to bind to the same antigen presenting molecule. The SW480 cell line has been found to exhibit only low expression of MHC class I alleles (Y. H. Liang et al., 2021). Therefore, co-culturing these cells represents limited antigen presentation and hence TCR interactions, which could explain the lack of change in activation in our experimental compared to control models. On the contrary, Jurkat cells are essentially cancer cells, and the physiological relevance of the mutations present in Jurkat cells raises a potential confounder. Importantly, Jurkat cells are deficient in phosphatase and tensin homologue (PTEN) which causes hyperresponsiveness to CD3 stimulation and premature priming of TCR signalling pathways (Shan et al., 2000). Further stimulation with PMA and ionomycin might have caused over-activation of calcium signalling pathways in these Jurkat cells and it can be argued that they have reached their upper limit of activation upon co-culturing with tumour spheroids, hence why the effect of *ATOH1*+ and SATB2-KO spheroids cannot be observed.

Future directions:

Further experiments can be performed to validate the findings in this study. First, the effect of *ATOH1* overexpression and SATB2-KO were only tested on two MSS cell lines SW480 and HT29. With more time, this can be replicated in other CRC cell lines, including MSI-H lines to compare the immune phenotype of these as a positive control, considering MSI-H cells are usually associated with enhanced immune response. Instead of Jurkat cells, primary allogenic T cells would serve as a better model for co-culture to test for immune response, as they have more robust TCR signalling and retain cytotoxic abilities (Dijkstra et al., 2018), unlike Jurkat cells. Furthermore, additional methods of measuring chemotaxis of immune cells such as a migration assay or live microscopy could be performed to validate the current findings.

Now that I have established methods to generate Paneth cell differentiation in CRC cell lines, future work could aim to replicate Paneth-like cell phenotype in CRC patient-derived organoids (PDOs) or genetically modified normal colon organoids (GMNCO). PDOs are able to mimic the biological characteristics and heterogeneity of primary tumours of patients (Vlachogiannis et al., 2018). The effects of *ATOH1* overexpression or SATB2 knockout on PDOs will be beneficial to decipher the complex mechanisms that might influence Paneth cell differentiation in the tumour. I began to work with GMNCOs to trial *ATOH1* overexpression but unfortunately these experiments had to stopped due to time constraints.

In this study, I was able to show that induction of Paneth cell differentiation may improve tumour immunogenicity. Therefore, Paneth-like cell differentiated PDOs

could be subsequently co-cultured with autologous T cells and T cell activation and proliferation assays performed to better understand whether a Paneth cell phenotype affects the interaction between T cells and cancer cells. Furthermore, the co-culture system presented in this work only considers the role of Jurkat cells, which are T cell mimic, whereas previous research has been discussing the role of Paneth cell secretions on the attraction of other immune cells e.g., dendritic cells or macrophages (Grigat et al., 2007). In fact, there was a surprising increase in dendritic cell signature in our original *in-silico* analysis of Paneth cell gene enriched tumours (Lal et al., 2022). This shows that these cells might be the target effectors of Paneth cell differentiation. Dendritic cells are important antigen presenting cells that have been found to play a crucial role in CRC as they are an important link between the innate and adaptive immune systems. Advanced CRC tumours have been shown to inhibit the maturation of dendritic cells and even induce dendritic cells with regulatory functions (Hargadon, 2013). Therefore, I propose that the Paneth cell phenotypic models presented here can be used as fundamental models to investigate potential interactions and activation of other immune cells such as dendritic cells with the tumour.

Conclusions and significance:

In summary, I showed that the MSS and MSI cancer cell lines SW480, HT29 and RKO have different differentiation potential and status. Drug compounds targeting the Wnt and Notch signalling pathways were able to alter secretory cell lineage differentiation in both 2D and 3D spheroid conditions. The immune response, in the form of Jurkat cell infiltration and IL2 secretion, against MSS cancers can potentially be augmented via artificial expression of Paneth cell gene marker *DEFA5* through *ATOH1* overexpression and SATB2-KO. This finding is important as efficacy of immunotherapy in MSS CRC is limited and unpredictable. It could be envisaged that Paneth cell differentiation therapy may provide benefit in improving MSS tumour response to immunotherapy. The ability of Paneth cells to enhance the host immune response against colon cancers, will enable further study on the capacity to cause formation of Paneth cells within colon cancers to augment current immunotherapy options.

Acknowledgements

I would like to sincerely thank my supervisor Simon Buczacki for his constant direction and support throughout my project. He gave me the opportunity to explore my own research opinions and ideas, whilst providing adequate guidance I needed to successfully complete my experiments and thesis. Thank you also to other members of the Buczacki lab especially Nikhil Lal, Yi Zhou, Jack Flower, Amit Mandal and Dedrick Chan for teaching me and assisting me with experimental techniques in the lab. Special gratitude to my course mates Teofanija, Alexa, Aiyan, Kelly, Cedric and also my family for being my emotional support throughout this year.

Bibliography

Abraham, R. T., & Weiss, A. (2004a). Jurkat T cells and development of the T-cell receptor signalling paradigm. *Nature Reviews Immunology 2004 4:4*, *4*(4), 301–308.

Abraham, R. T., & Weiss, A. (2004b). Jurkat T cells and development of the T-cell receptor signalling paradigm. *Nature Reviews Immunology 2004 4:4*, *4*(4), 301–308.

Alcamí, J., de Lera, T. L., Folgueira, L., Pedraza, M. A., Jacqué, J. M., Bachelerie, F., Noriega, A. R., Hay, R. T., Harrich, D., Gaynor, R. B., Virelizier, J. L., & Arenzana-Seisdedos, F. (1995). Absolute dependence on kappa B responsive elements for initiation and Tat-mediated amplification of HIV transcription in blood CD4 T lymphocytes. *The EMBO Journal*, *14*(7), 1552–1560.

A. Treveil, P. Sudhakar, J. Matthews, Z., T. Wrzesiński, J. Jones, E., J. Brooks, M. Ölbei, I. Hautefort, J. Hall, L., R. Carding, S., U. Mayer, P. Powell, P., T. Wileman, Palma, F. D., W. Haerty, & T. Korcsmáros. (2020). Regulatory network analysis of Paneth cell and goblet cell enriched gut organoids using transcriptomics approaches. *Molecular Omics*, *16*(1), 39–58.

Barretina, J., Caponigro, G., Stransky, N., Venkatesan, K., Margolin, A. A., Kim, S., Wilson, C. J., Lehár, J., Kryukov, G. v., Sonkin, D., Reddy, A., Liu, M., Murray, L., Berger, M. F., Monahan, J. E., Morais, P., Meltzer, J., Korejwa, A., Jané-Valbuena, J., … Garraway, L. A. (2012). The Cancer Cell Line Encyclopedia enables predictive modelling of anticancer drug sensitivity. *Nature*, *483*(7391), 603–607.

Barreto e Barreto, L., Rattes, I. C., da Costa, A. V., & Gama, P. (2022). Paneth cells and their multiple functions. *Cell Biology International*.

Berg, K. C. G., Eide, P. W., Eilertsen, I. A., Johannessen, B., Bruun, J., Danielsen, S. A., Bjørnslett, M., Meza-Zepeda, L. A., Eknæs, M., Lind, G. E., Myklebost, O., Skotheim, R. I., Sveen, A., & Lothe, R. A. (2017). Multi-omics of 34 colorectal cancer cell lines - a resource for biomedical studies. *Molecular Cancer*, *16*(1), 1–16.

Bevins, C. L., & Salzman, N. H. (2011). Paneth cells, antimicrobial peptides and maintenance of intestinal homeostasis. *Nature Reviews Microbiology 2011 9:5*, *9*(5), 356–368.

Bickel, M. (1993). The role of interleukin-8 in inflammation and mechanisms of regulation. *J Periodontol*, 64(5 Suppl), 456-60.

Boyman, O., & Sprent, J. (2012). The role of interleukin-2 during homeostasis and activation of the immune system. *Nature Reviews Immunology 2012 12:3*, *12*(3), 180–190.

Brennan, D. J., Naicker, K., Das, S., Moran, B., Klinger, R., Ponten, F., Hewitt, S., Jirström, K., Byrne, A. T., O'Sullivan, J., Gallagher, W. M., & O'Connor, D. P. (2019). Abstract 5033: The role of the epigenetic regulator SATB2 in colon cancer progression. *Cancer Research*, *79*(13_Supplement), 5033–5033.

Burclaff, J., Bliton, R. J., Breau, K. A., Ok, M. T., Gomez-Martinez, I., Ranek, J. S., Bhatt, A. P., Purvis, J. E., Woosley, J. T., & Magness, S. T. (2022a). A Proximal-to-Distal Survey of Healthy Adult Human Small Intestine and Colon Epithelium by Single-Cell Transcriptomics. *CMGH*, *13*(5), 1554–1589.

Burclaff, J., Bliton, R. J., Breau, K. A., Ok, M. T., Gomez-Martinez, I., Ranek, J. S., Bhatt, A. P., Purvis, J. E., Woosley, J. T., & Magness, S. T. (2022b). A Proximal-

to-Distal Survey of Healthy Adult Human Small Intestine and Colon Epithelium by Single-Cell Transcriptomics. *Cellular and Molecular Gastroenterology and Hepatology*, *13*(5), 1554–1589.

Cerami, E., Gao, J., Dogrusoz, U., Gross, B. E., Sumer, S. O., Aksoy, B. A., Jacobsen, A., Byrne, C. J., Heuer, M. L., Larsson, E., Antipin, Y., Reva, B., Goldberg, A. P., Sander, C., & Schultz, N. (2012). The cBio Cancer Genomics Portal: An Open Platform for Exploring Multidimensional Cancer Genomics Data. *Cancer Discovery*, *2*(5), 401–404.

Chan, D. K. H., & Buczacki, S. J. A. (2021). Tumour heterogeneity and evolutionary dynamics in colorectal cancer. *Oncogenesis 2021 10:7*, *10*(7), 1–9.

Clipstone, N. A., & Crabtree, G. R. (1992). Identification of calcineurin as a key signalling enzyme in T-lymphocyte activation. *Nature 1992 357:6380*, *357*(6380), 695–697.

Costa, E. C., Moreira, A. F., de Melo-Diogo, D., Gaspar, V. M., Carvalho, M. P., & Correia, I. J. (2016). 3D tumor spheroids: an overview on the tools and techniques used for their analysis. *Biotechnology Advances*, *34*(8), 1427–1441.

de Leeuw, E., Burks, S. R., Li, X., Kao, J. P. Y., & Lu, W. (2007). Structure-dependent functional properties of Human Defensin 5. *FEBS Letters*, *581*(3), 515.

Dijkstra, K. K., Cattaneo, C. M., Weeber, F., Chalabi, M., van de Haar, J., Fanchi, L. F., Slagter, M., van der Velden, D. L., Kaing, S., Kelderman, S., van Rooij, N., van Leerdam, M. E., Depla, A., Smit, E. F., Hartemink, K. J., de Groot, R., Wolkers, M. C., Sachs, N., Snaebjornsson, P., … Voest, E. E. (2018). Generation of Tumor-Reactive T Cells by Co-culture of Peripheral Blood Lymphocytes and Tumor Organoids. *Cell*, *174*(6), 1586-1598.e12.

Du, W., Frankel, T. L., Green, M., & Zou, W. (2021). IFNγ signaling integrity in colorectal cancer immunity and immunotherapy. *Cellular & Molecular Immunology 2021 19:1*, *19*(1), 23–32.

Durand, A., Donahue, B., Peignon, G., Letourneur, F., Cagnard, N., Slomianny, C., Perret, C., Shroyer, N. F., & Romagnolo, B. (2012a). Functional intestinal stem cells after Paneth cell ablation induced by the loss of transcription factor Math1 (Atoh1). *Proceedings of the National Academy of Sciences of the United States of America*, *109*(23), 8965–8970.

Durand, A., Donahue, B., Peignon, G., Letourneur, F., Cagnard, N., Slomianny, C., Perret, C., Shroyer, N. F., & Romagnolo, B. (2012b). Functional intestinal stem cells after Paneth cell ablation induced by the loss of transcription factor Math1 (Atoh1). *Proceedings of the National Academy of Sciences of the United States of America*, *109*(23), 8965–8970.

Eberhard, J., Gaber, A., Wangefjord, S., Nodin, B., Uhlén, M., Ericson Lindquist, K., & Jirström, K. (2012). A cohort study of the prognostic and treatment predictive value of SATB2 expression in colorectal cancer. *British Journal of Cancer*, *106*(5), 931.

Edmondson, R., Broglie, J. J., Adcock, A. F., & Yang, L. (2014). Three-Dimensional Cell Culture Systems and Their Applications in Drug Discovery and Cell-Based Biosensors. *Assay and Drug Development Technologies*, *12*(4), 207.

Farin, H. F., van Es, J. H., & Clevers, H. (2012). Redundant sources of Wnt regulate intestinal stem cells and promote formation of paneth cells. *Gastroenterology*, *143*(6).

Fearon, E. R., & Vogelstein, B. (1990). A genetic model for colorectal tumorigenesis. *Cell*, *61*(5), 759–767.

Foo, C. C., Ku, C., Wei, R., Yip, J., Tsang, J., Chan, T. Y., Lo, O., & Law, W. L. (2020). How does lymph node yield affect survival outcomes of stage I and II colon cancer? *World Journal of Surgical Oncology 2020 18:1*, *18*(1), 1–8.

Gao, J., Aksoy, B. A., Dogrusoz, U., Dresdner, G., Gross, B., Sumer, S. O., Sun, Y., Jacobsen, A., Sinha, R., Larsson, E., Cerami, E., Sander, C., & Schultz, N. (2013). Integrative analysis of complex cancer genomics and clinical profiles using the cBioPortal. *Science Signaling*, *6*(269).

Gao, S., Yan, L., Wang, R., Li, J., Yong, J., Zhou, X., Wei, Y., Wu, X., Wang, X., Fan, X., Yan, J., Zhi, X., Gao, Y., Guo, H., Jin, X., Wang, W., Mao, Y., Wang, F., Wen, L., … Tang, F. (2018). Tracing the temporal-spatial transcriptome landscapes of the human fetal digestive tract using single-cell RNA-sequencing. *Nature Cell Biology 2018 20:6*, *20*(6), 721–734.

Grigat, J., Soruri, A., Forssmann, U., Riggert, J., & Zwirner, J. (2007). Chemoattraction of Macrophages, T Lymphocytes, and Mast Cells Is Evolutionarily Conserved within the Human α-Defensin Family. *The Journal of Immunology*, *179*(6), 3958–3965.

Gu, W., Wang, H., Huang, X., Kraiczy, J., Singh, P. N. P., Ng, C., Dagdeviren, S., Houghton, S., Pellon-Cardenas, O., Lan, Y., Nie, Y., Zhang, J., Banerjee, K. K., Onufer, E. J., Warner, B. W., Spence, J., Scherl, E., Rafii, S., Lee, R. T., … Zhou, Q. (2021). SATB2 preserves colon stem cell identity and mediates ileum-colon conversion via enhancer remodeling. *Cell Stem Cell*, 29 (1).

Guinney, J., Dienstmann, R., Wang, X., de Reyniès, A., Schlicker, A., Soneson, C., Marisa, L., Roepman, P., Nyamundanda, G., Angelino, P., Bot, B. M., Morris, J. S., Simon, I. M., Gerster, S., Fessler, E., de Sousa .E Melo, F., Missiaglia, E., Ramay, H., Barras, D., … Tejpar, S. (2015). The consensus molecular subtypes of colorectal cancer. *Nature Medicine 2015 21:11*, *21*(11), 1350–1356.

Halsted, W. S. (1907). I. The Results of Radical Operations for the Cure of Carcinoma of the Breast. *Annals of Surgery*, *46*(1), 1.

HALSTED, W. S. M. D. . (1894). THE RESULTS OF OPERATIONS FOR THE CURE OF CANCER OF THE BREA... : Annals of Surgery. *Annals of Surgery*, *20*, 497–555.

Hargadon, K. M. (2013). Tumor-Altered Dendritic Cell Function: Implications for Anti-Tumor Immunity. *Frontiers in Immunology*, *4*(JUL).

Hiramatsu, Y., Fukuda, A., Ogawa, S., Goto, N., Ikuta, K., Tsuda, M., Matsumoto, Y., Kimura, Y., Yoshioka, T., Takada, Y., Maruno, T., Hanyu, Y., Tsuruyama, T., Wang, Z., Akiyama, H., Takaishi, S., Miyoshi, H., Taketo, M. M., Chiba, T., & Seno, H. (2019). Arid1a is essential for intestinal stem cells through Sox9 regulation. *Proceedings of the National Academy of Sciences of the United States of America*, *116*(5), 1704–1713.

Holmes, E. J. (1965). Neoplastic paneth cells their occurrence in 2 adenomas and one carcinoma of the colon. *Cancer*, 15, 1416-1422.

Ionov, Y., Peinado, M. A., Malkhosyan, S., Shibata, D., & Perucho, M. (1993). Ubiquitous somatic mutations in simple repeated sequences reveal a new mechanism for colonic carcinogenesis. *Nature 1993 363:6429*, *363*(6429), 558–561.

Ishikawa, C., Tanabe, H., Maemoto, A., Ito, T., Watari, J., Kono, T., Fujiya, M., Ashida, T., Ayabe, T., & Kohgo, Y. (2010). Precursor Processing of Human Defensin-5 Is Essential to the Multiple Functions in vitro and in vivo. *Journal of Innate Immunity*, *2*(1), 66–76.

Ito, T., Tanabe, H., Ayabe, T., Ishikawa, C., Inaba, Y., Maemoto, A., Kono, T., Ashida, T., Fujiya, M., & Kohgo, Y. (2012). Paneth Cells Regulate Both Chemotaxis of Immature Dendritic Cells and Cytokine Production from Epithelial Cells. *The Tohoku Journal of Experimental Medicine*, *227*(1), 39–48.

Kazanjian, A., & Shroyer, N. F. (2011). NOTCH Signaling and ATOH1 in Colorectal Cancers. *Current Colorectal Cancer Reports 2011 7:2*, *7*(2), 121–127.

Lal, N., Chan, D. K. H., Ng, M. E., Vermeulen, L., & Buczacki, S. J. A. (2022). Primary tumour immune response and lymph node yields in colon cancer. *British Journal of Cancer 2022 126:8*, *126*(8), 1178–1185.

Le, D. T., Uram, J. N., Wang, H., Bartlett, B. R., Kemberling, H., Eyring, A. D., Skora, A. D., Luber, B. S., Azad, N. S., Laheru, D., Biedrzycki, B., Donehower, R. C., Zaheer, A., Fisher, G. A., Crocenzi, T. S., Lee, J. J., Duffy, S. M., Goldberg, R. M., de la Chapelle, A., … Diaz, L. A. (2015). PD-1 Blockade in Tumors with Mismatch-Repair Deficiency. *The New England Journal of Medicine*, *372*(26), 2509.

le Voyer, T. E., Sigurdson, E. R., Hanlon, A. L., Mayer, R. J., Macdonald, J. S., Catalano, P. J., & Haller, D. G. (2003). Colon cancer survival is associated with increasing number of lymph nodes analyzed: A secondary survey of intergroup trial INT-0089. *Journal of Clinical Oncology*, *21*(15), 2912–2919.

Leow, C. C., Romero, M. S., Ross, S., Polakis, P., & Gao, W. Q. (2004). Hath1, Down-Regulated in Colon Adenocarcinomas, Inhibits Proliferation and Tumorigenesis of Colon Cancer Cells. *Cancer Research*, *64*(17), 6050–6057.

Li, C., Wang, Y., Gong, Y., Zhang, T., Huang, J., Tan, Z., & Xue, L. (2021). Finding an easy way to harmonize: a review of advances in clinical research and combination strategies of EZH2 inhibitors. *Clinical Epigenetics*, *13*(1), 1–12.

Liang, X., Duronio, G. N., Yang, Y., Bala, P., Hebbar, P., Spisak, S., Sahgal, P., Singh, H., Zhang, Y., Xie, Y., Cejas, P., Long, H. W., Bass, A. J., & Sethi, N. S. (2022). An Enhancer-Driven Stem Cell–Like Program Mediated by SOX9 Blocks Intestinal Differentiation in Colorectal Cancer. *Gastroenterology*, *162*(1), 209–222.

Liang, Y. H., Tsai, J. H., Cheng, Y. M., Chan, K. Y., Hsu, W. L., Lee, C. C., Chen, K. H., & Yeh, K. H. (2021). Chemotherapy agents stimulate dendritic cells against human colon cancer cells through upregulation of the transporter associated with antigen processing. *Scientific Reports 2021 11:1*, *11*(1), 1–13.

Lin, A., Zhang, J., & Luo, P. (2020). Crosstalk Between the MSI Status and Tumor Microenvironment in Colorectal Cancer. *Frontiers in Immunology*, *11*, 2039.

Lisitsyn, N. A., Bukurova, Y. A., Nikitina, I. G., Krasnov, G. S., Sykulev, Y., & Beresten, S. F. (2012). Enteric alpha defensins in norm and pathology. *Annals of Clinical Microbiology and Antimicrobials*, *11*, 1.

Lo, Y. H., Chung, E., Li, Z., Wan, Y. W., Mahe, M. M., Chen, M. S., Noah, T. K., Bell, K. N., Yalamanchili, H. K., Klisch, T. J., Liu, Z., Park, J. S., & Shroyer, N. F. (2017). Transcriptional Regulation by ATOH1 and its Target SPDEF in the Intestine. *CMGH*, *3*(1), 51–71.

López-Arribillaga, E., Yan, B., Lobo-Jarne, T., Guillén, Y., Menéndez, S., Andreu, M., Bigas, A., Iglesias, M., & Espinosa, L. (2021). Accumulation of paneth cells in early colorectal adenomas is associated with beta-catenin signaling and poor patient prognosis. *Cells*, *10*(11).

M, B. (1993). The role of interleukin-8 in inflammation and mechanisms of regulation - PubMed. *J Periodontol*, *May*(64(5 Suppl)), 456–460.

Mahon, M., Xu, J., Yi, X., Liu, X., Gao, N., & Zhang, L. (2016). Paneth Cell in Adenomas of the Distal Colorectum Is Inversely Associated with Synchronous Advanced Adenoma and Carcinoma. *Scientific Reports 2016 6:1*, *6*(1), 1–7.

Mantani, Y., Nishida, M., Yuasa, H., Yamamoto, K., Takahara, E. I., Omotehara, T., Udayanga, K. G. S., Kawano, J., Yokoyama, T., Hoshi, N., & Kitagawa, H. (2014). Ultrastructural and Histochemical Study on the Paneth Cells in the Rat Ascending Colon. *The Anatomical Record*, *297*(8), 1462–1471.

Martin-Hijano, L., & Sainz, B. (2020). The Interactions Between Cancer Stem Cells and the Innate Interferon Signaling Pathway. *Frontiers in Immunology*, *11*, 526.

Naito, Y., Saito, K., Shiiba, K., Ohuchi, A., Saigenji, K., Nagura, H., & Ontani1, H. (1998). CD8+ T Cells Infiltrated within Cancer Cell Nests as a Prognostic Factor in Human Colorectal Cancer. *CANCER RESEARCH*, *58*, 3491–3494.

Nakanishi, Y., Reina-Campos, M., Nakanishi, N., Llado, V., Elmen, L., Peterson, S., Campos, A., De, S. K., Leitges, M., Ikeuchi, H., Pellecchia, M., Blumberg, R. S., Diaz-Meco, M. T., & Moscat, J. (2016). Control of Paneth Cell Fate, Intestinal Inflammation, and Tumorigenesis by PKCλ/ι. *Cell Reports*, *16*(12), 3297–3310.

Ostrop, J., Zwiggelaar, R. T., Terndrup Pedersen, M., Gerbe, F., Bösl, K., Lindholm, H. T., Díez-Sánchez, A., Parmar, N., Radetzki, S., von Kries, J. P., Jay, P., Jensen, K. B., Arrowsmith, C., & Oudhoff, M. J. (2021). A Semi-automated Organoid Screening Method Demonstrates Epigenetic Control of Intestinal Epithelial Differentiation. *Frontiers in Cell and Developmental Biology*, *8*, 1797.

Overman, M. J., Lonardi, S., Wong, K. Y. M., Lenz, H. J., Gelsomino, F., Aglietta, M., Morse, M. A., van Cutsem, E., McDermott, R., Hill, A., Sawyer, M. B., Hendlisz, A., Neyns, B., Svrcek, M., Moss, R. A., Ledeine, J. M., Cao, Z. A., Kamble, S., Kopetz, S., & André, T. (2018). Durable Clinical Benefit With Nivolumab Plus Ipilimumab in DNA Mismatch Repair-Deficient/Microsatellite Instability-High Metastatic Colorectal Cancer. *Journal of Clinical Oncology : Official Journal of the American Society of Clinical Oncology*, *36*(8), 773–779.

Overman, M. J., McDermott, R., Leach, J. L., Lonardi, S., Lenz, H. J., Morse, M. A., Desai, J., Hill, A., Axelson, M., Moss, R. A., Goldberg, M. v., Cao, Z. A., Ledeine, J. M., Maglinte, G. A., Kopetz, S., & André, T. (2017). Nivolumab in patients with metastatic DNA mismatch repair deficient/microsatellite instability–high colorectal cancer (CheckMate 142): results of an open-label, multicentre, phase 2 study. *The Lancet. Oncology*, *18*(9), 1182.

Pai, R. K., Rybicki, L. A., Goldblum, J. R., Shen, B., Xiao, S. Y., & Liu, X. (2013). Paneth cells in colonic adenomas: Association with male sex and adenoma burden. *American Journal of Surgical Pathology*, *37*(1), 98–103.

Pelka, K., Hofree, M., Chen, J. H., Sarkizova, S., Pirl, J. D., Jorgji, V., Bejnood, A., Dionne, D., Ge, W. H., Xu, K. H., Chao, S. X., Zollinger, D. R., Lieb, D. J., Reeves, J. W., Fuhrman, C. A., Hoang, M. L., Delorey, T., Nguyen, L. T., Waldman, J., … Hacohen, N. (2021). Spatially organized multicellular immune hubs in human colorectal cancer. *Cell*, *184*(18), 4734-4752.e20.

Pflügler, S., Svinka, J., Scharf, I., Crncec, I., Filipits, M., Charoentong, P., Tschurtschenthaler, M., Kenner, L., Awad, M., Stift, J., Schernthanner, M., Bischl, R., Herndler-Brandstetter, D., Glitzner, E., Moll, H. P., Casanova, E., Timelthaler, G., Sibilia, M., Gnant, M., … Eferl, R. (2020). IDO1+ Paneth cells promote immune escape of colorectal cancer. *Communications Biology*, *3*(1).

Pino, M. S., & Chung, D. C. (2010). The Chromosomal Instability Pathway in Colon Cancer. *Gastroenterology*, *138*(6), 2059–2072.

Prall, F., Dührkop, T., Weirich, V., Ostwald, C., Lenz, P., Nizze, H., & Barten, M. (2004). Prognostic role of CD8+ tumor-infiltrating lymphocytes in stage III colorectal cancer with and without microsatellite instability. *Human Pathology*, *35*(7), 808–816.

Raskov, H., Orhan, A., Christensen, J. P., & Gögenur, I. (2020). Cytotoxic CD8+ T cells in cancer and cancer immunotherapy. *British Journal of Cancer 2020 124:2*, *124*(2), 359–367.

Rosenberg, S. A. (2014). IL-2: The First Effective Immunotherapy for Human Cancer. *Journal of Immunology (Baltimore, Md. : 1950)*, *192*(12), 5451.

Rothenberg, M. E., Nusse, Y., Kalisky, T., Lee, J. J., Dalerba, P., Scheeren, F., Lobo, N., Kulkarni, S., Sim, S., Qian, D., Beachy, P. A., Pasricha, P. J., Quake, S. R., & Clarke, M. F. (2012). Identification of a cKit(+) colonic crypt base secretory cell that supports Lgr5(+) stem cells in mice. *Gastroenterology*, *142*(5).

Sansom, O. J., Reed, K. R., Hayes, A. J., Ireland, H., Brinkmann, H., Newton, I. P., Batlle, E., Simon-Assmann, P., Clevers, H., Nathke, I. S., Clarke, A. R., & Winton, D. J. (2004). Loss of Apc in vivo immediately perturbs Wnt signaling, differentiation, and migration. *Genes & Development*, *18*(12), 1385.

Sarli, L., Bader, G., Iusco, D., Salvemini, C., di Mauro, D., Mazzeo, A., Regina, G., & Roncoroni, L. (2005). Number of lymph nodes examined and prognosis of TNM stage II colorectal cancer. *European Journal of Cancer*, *41*(2), 272–279.

Sato, T., van Es, J. H., Snippert, H. J., Stange, D. E., Vries, R. G., van den Born, M., Barker, N., Shroyer, N. F., van de Wetering, M., & Clevers, H. (2011). Paneth cells constitute the niche for Lgr5 stem cells in intestinal crypts. *Nature*, *469*(7330), 415–418.

Schneider, U., Schwenk, H. -U, & Bornkamm, G. (1977). Characterization of EBV-genome negative “null” and “T” cell lines derived from children with acute lymphoblastic leukemia and leukemic transformed non-Hodgkin lymphoma. *International Journal of Cancer*, *19*(5), 621–626.

Serra, D., Mayr, U., Boni, A., Lukonin, I., Rempfler, M., Challet Meylan, L., Stadler, M. B., Strnad, P., Papasaikas, P., Vischi, D., Waldt, A., Roma, G., & Liberali, P. (2019). Self-organization and symmetry breaking in intestinal organoid development. *Nature*, *569*(7754), 66–72.

Shan, X., Czar, M. J., Bunnell, S. C., Liu, P., Liu, Y., Schwartzberg, P. L., & Wange, R. L. (2000). Deficiency of PTEN in Jurkat T Cells Causes Constitutive Localization of Itk to the Plasma Membrane and Hyperresponsiveness to CD3 Stimulation. *Molecular and Cellular Biology*, *20*(18), 6945–6957.

Simmonds, N., Furman, M., Karanika, E., Phillips, A., & Bates, A. W. H. (2014). Paneth cell metaplasia in newly diagnosed inflammatory bowel disease in children. *BMC Gastroenterology*, *14*(1), 93.

Sottoriva, A., Cresswell, G., Spiteri, I., Lynn, C., Fernandez-Mateos, J., Zapata, L., Chkhaidze, K., Nichol, D., James, C., Mossner, M., Kimberley, C., Househam, J., Berner, A., & Schmidt, M. (2021). *The co-evolution of the genome and epigenome in colorectal cancer*.

Sottoriva, A., Kang, H., Ma, Z., Graham, T. A., Salomon, M. P., Zhao, J., Marjoram, P., Siegmund, K., Press, M. F., Shibata, D., & Curtis, C. (2015). A Big Bang model of human colorectal tumor growth. *Nature Genetics 2015 47:3*, *47*(3), 209–216.

Turgeon, N., Blais, M., Gagné, J. M., Tardif, V., Boudreau, F., Perreault, N., & Asselin, C. (2013). HDAC1 and HDAC2 Restrain the Intestinal Inflammatory

Response by Regulating Intestinal Epithelial Cell Differentiation. *PLOS ONE*, *8*(9), e73785.

VanDussen, K. L., & Samuelson, L. C. (2010). Mouse Atonal Homolog 1 Directs Intestinal Progenitors to Secretory Cell Rather than Absorptive Cell Fate. *Developmental Biology*, *346*(2), 215.

Vlachogiannis, G., Hedayat, S., Vatsiou, A., Jamin, Y., Fernández-Mateos, J., Khan, K., Lampis, A., Eason, K., Huntingford, I., Burke, R., Rata, M., Koh, D. M., Tunariu, N., Collins, D., Hulkki-Wilson, S., Ragulan, C., Spiteri, I., Moorcraft, S. Y., Chau, I., … Valeri, N. (2018). Patient-derived organoids model treatment response of metastatic gastrointestinal cancers. *Science (New York, N.Y.)*, *359*(6378), 920.

Wang, Y., Wang, M., & Li, Y. (2016). Anti-colorectal cancer effect of interleukin-2 and interferon-β fusion gene driven by carcinoembryonic antigen promoter. *OncoTargets and Therapy*, *9*, 3259.

Wang, Z., Jensen, M. A., & Zenklusen, J. C. (2016). A practical guide to The Cancer Genome Atlas (TCGA). *Methods in Molecular Biology*, *1418*, 111–141.

Wehkamp, J., Salzman, N. H., Porter, E., Nuding, S., Weichenthal, M., Petras, R. E., Shen, B., Schaeffeler, E., Schwab, M., Linzmeier, R., Feathers, R. W., Chu, H., Lima, H., Fellermann, K., Ganz, T., Stange, E. F., & Bevins, C. L. (2005). Reduced Paneth cell α-defensins in ileal Crohn's disease. *Proceedings of the National Academy of Sciences of the United States of America*, *102*(50), 18129.

Weiss, A., Wiskocil, R. L., & Stobo, J. D. (1984). The role of T3 surface molecules in the activation of human T cells: a two-stimulus requirement for IL 2 production reflects events occurring at a pre-translational level. *The Journal of Immunology*, *133*(1).

Xi, Y., & Xu, P. (2021). Global colorectal cancer burden in 2020 and projections to 2040. *Translational Oncology*, *14*(10), 101174.

Xian, L., Georgess, D., Huso, T., Cope, L., Belton, A., Chang, Y.-T., Kuang, W., Gu, Q., Zhang, X., Senger, S., Fasano, A., Huso, D. L., Ewald, A. J., & Resar, L. M. S. (2017). HMGA1 amplifies Wnt signalling and expands the intestinal stem cell compartment and Paneth cell niche. *Nature Communications 2017 8:1*, *8*(1), 1–15.

Xu, Y. J., Zhao, J. M., Gao, C., Ni, X. F., Wang, W., Hu, W. W., & Wu, C. P. (2021). Hsa_circ_0136666 activates Treg-mediated immune escape of colorectal cancer via miR-497/PD-L1 pathway. *Cellular Signalling*, *86*, 110095.

Yilmaz, Ö. H., Katajisto, P., Lamming, D. W., Gültekin, Y., Bauer-Rowe, K. E., Sengupta, S., Birsoy, K., Dursun, A., Onur Yilmaz, V., Selig, M., Nielsen, G. P., Mino-Kenudson, M., Zukerberg, L. R., Bhan, A. K., Deshpande, V., & Sabatini, D. M. (2012). MTORC1 in the Paneth cell niche couples intestinal stem-cell function to calorie intake. *Nature*, *486*(7404), 490–495.

Yin, X., Farin, H. F., van Es, J. H., Clevers, H., Langer, R., & Karp, J. M. (2014). Niche-independent high-purity cultures of Lgr5 + intestinal stem cells and their progeny. *Nature Methods*, *11*(1), 106–112.

Zhao, B., Zhao, H., & Zhao, J. (2020). Efficacy of PD-1/PD-L1 blockade monotherapy in clinical trials. *Therapeutic Advances in Medical Oncology*, *12*.

Zheng, Y., Fang, Y. C., & Li, J. (2019). PD-L1 expression levels on tumor cells affect their immunosuppressive activity. *Oncology Letters*, *18*(5), 5399.

Zhou, L., Mudianto, T., Ma, X., Riley, R., & Uppaluri, R. (2020). Targeting EZH2 enhances antigen presentation, antitumor immunity, and circumvents anti–PD-

1 resistance in head and neck cancer. *Clinical Cancer Research*, *26*(1), 290–300.

Zwiggelaar, R. T., Lindholm, H. T., Fosslie, M., Pedersen, M. T., Ohta, Y., Díez-Sánchez, A., Martín-Alonso, M., Ostrop, J., Matano, M., Parmar, N., Kvaløy, E., Spanjers, R. R., Nazmi, K., Rye, M., Drabløs, F., Arrowsmith, C., Dahl, J. A., Jensen, K. B., Sato, T., & Oudhoff, M. J. (2020). LSD1 represses a neonatal/reparative gene program in adult intestinal epithelium. *Science Advances*, *6*(37), 14.